DTIC FILE COPY

(4)

SEC

ORT DOCUMENTATION PAGE

1a. **AD-A198 070**

1b. RESTRICTIVE MARKINGS
None

2a. SECURITY CLASSIFICATION

3. DISTRIBUTION/AVAILABILITY OF REPORT
Unlimited

2b. DECLASSIFICATION/DOWNGRADING SCHEDULE

4. PERFORMING ORGANIZATION REPORT NUMBER(S)
Interim Technical Report # 22

5. MONITORING ORGANIZATION REPORT NUMBER(S)

6a. NAME OF PERFORMING ORGANIZATION
Department of Chemistry

6b. OFFICE SYMBOL (If applicable)

7a. NAME OF MONITORING ORGANIZATION
Office of Naval Research

6c. ADDRESS (City, State, and ZIP Code)
Massachusetts Institute of Technology
77 Mass. Avenue, Bldg. 6-335
Cambridge, MA 02139

7b. ADDRESS (City, State, and ZIP Code)
Chemistry Division
800 N. Quincy Street
Arlington, VA 22217

8a. NAME OF FUNDING/SPONSORING ORGANIZATION
Office of Naval Research

8b. OFFICE SYMBOL (If applicable)

9. PROCUREMENT INSTRUMENT IDENTIFICATION NUMBER
N00014-84-K-0553

8c. ADDRESS (City, State, and ZIP Code)
Chemistry division
800 N. Quincy Street
Arlington, VA 22217

10. SOURCE OF FUNDING NUMBERS

PROGRAM ELEMENT NO.	PROJECT NO.	TASK NO.	WORK UNIT ACCESSION NO.
		051-579	

11. TITLE (Include Security Classification)
Synthesis and Charge Transport Properties of Polymers Derived from Oxidation of 1-H-1'(6-pyrrol-1-yl)-hexyl-4,4'-bipyridinium.....

12. PERSONAL AUTHOR(S)
Ching-Fong Shu and Mark S. Wrighton

13a. TYPE OF REPORT	13b. TIME COVERED	14. DATE OF REPORT (Year, Month, Day)	15. PAGE COUNT
technical interim	FROM _____ TO _____	August 15, 1988	55

16. SUPPLEMENTARY NOTATION
Prepared for Publication in the Journal of Physical Chemistry

17. COSATI CODES			18. SUBJECT TERMS (Continue on reverse if necessary and identify by block number)
FIELD	GROUP	SUB-GROUP	Microelectrode array, redox polymer, polypyrrole, viologen

19. ABSTRACT (Continue on reverse if necessary and identify by block number)

See Attached Sheet

20. DISTRIBUTION/AVAILABILITY OF ABSTRACT
☐ UNCLASSIFIED/UNLIMITED ☐ SAME AS RPT. ☐ DTIC USERS

21. ABSTRACT SECURITY CLASSIFICATION
Unlimited

22a. NAME OF RESPONSIBLE INDIVIDUAL
Mark S. Wrighton

22b. TELEPHONE (Include Area Code)
617-253-1597

22c. OFFICE SYMBOL

DD FORM 1473, 84 MAR

83 APR edition may be used until exhausted.
All other editions are obsolete.

SECURITY CLASSIFICATION OF THIS PAGE

Abstract

This article describes the synthesis and electrochemical properties of redox polymers, having a polypyrrole backbone and viologen subunits, derived from oxidative electropolymerization of 1-methyl-1'-(6-pyrrol-1-yl)-hexyl-4,4'-bipyridinium, (P-V-$Me^{2+}_{\square}$), and 1-H-1'-(6-pyrrol-1-yl)-hexyl-4,4'-bipyridinium, (P-V-$H^{2+}_{\square}$). Closely spaced (≤1.5 μm) Au microelectrode arrays (≤2.5 μm wide x 50 μm long x 0.1 μm high) modified with the polymers can be used to study aspects of the charge transport behavior of the viologen redox system. Poly(P-V-$Me^{2+}_{\square}$) and poly(P-V-$H^{2+}_{\square}$) have been used to investigate the characteristics of microelectrochemical transistors based on a viologen redox center, and a similar redox center, protonated, mono-quaternized bipyridinium, which is pH dependent. The interesting properties from Poly(P-V-Me^{2+}) and poly(P-V-H^{2+}) stem from the behavior of the pendant viologen redox centers. The device based on poly(P-V-Me^{2+}) has a narrow region (~200 mV) of gate voltage, V_G, where the source-drain current, I_D, is non-zero and has a sharp, pH-independent peak in the I_D-V_G plot at ~-0.53 V vs. SCE associated with the reversible, one-electron reduction of viologen. This result is consistent with electron self-exchange between redox centers being the mechanism for charge transport. The device based on poly(P-V-H^{2+}) shows a pH-dependent I_D at fixed V_G, as expected from the electrochemical behavior from reversible protonation of the terminal N of the bipyridinium

group of poly(P-V-H^{2+}). The microelectrochemical transistor based on poly(P-V-H^{2+}) illustrates the design of chemically sensitive, molecule-based devices using conventional redox materials.

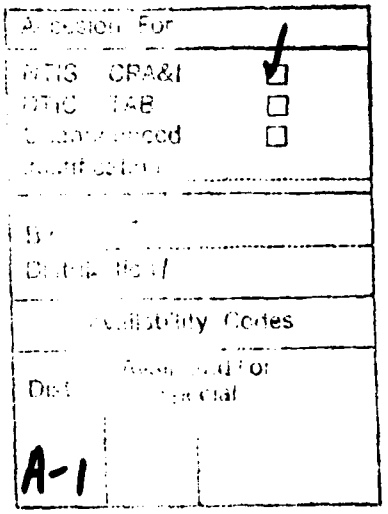

Office of Naval Research

Contract N00014-84-K-0553

Task No. 051-579

Technical Report #22

Synthesis and Carge Transport Properties of Polymers Derived from Oxidation of 1-H-1'(6-pyrrol-1-yl)-hexyl-4,4'-bipyridinium Bis-hexafluorophosphate and Demonstration of a pH Sensitive Microelectrochemical Transistor Derived from the Redox Properties of a Conventional Redox Center

by

Ching-Fong Shu and Mark S. Wrighton

Department of Chemistry
Massachusetts Institute of Technology
Cambridge, MA 02139

Prepared for Publication in

Journal of Physical Chemistry

August 15, 1988

[Prepared for publication in the Journal of Physical Chemistry]

Synthesis and Charge Transport Properties of Polymers Derived from Oxidation of 1-H-1'-(6-pyrrol-1-yl)-hexyl-4,4'-bipyridinium Bis-hexafluorophosphate and Demonstration of a pH Sensitive Microelectrochemical Transistor Derived from the Redox Properties of a Conventional Redox Center

Ching-Fong Shu and Mark S. Wrighton*

Department of Chemistry
Massachusetts Institute of Technology
Cambridge, Massachusetts 02139

*Author to whom inquires are to be addressed.

Abstract

This article describes the synthesis and electrochemical properties of redox polymers, having a polypyrrole backbone and viologen subunits, derived from oxidative electropolymerization of 1-methyl-1'-(6-pyrrol-1-yl)-hexyl-4,4'-bipyridinium, ($P\text{-}V\text{-}Me^{2+}$), and 1-H-1'-(6-pyrrol-1-yl)-hexyl-4,4'-bipyridinium, ($P\text{-}V\text{-}H^{2+}$). Closely spaced (~1.5 μm) Au microelectrode arrays (~2.5 μm wide x 50 μm long x 0.1 μm high) modified with the polymers can be used to study aspects of the charge transport behavior of the viologen redox system. Poly($P\text{-}V\text{-}Me^{2+}$) and poly($P\text{-}V\text{-}H^{2+}$) have been used to investigate the characteristics of microelectrochemical transistors based on a viologen redox center, and a similar redox center, protonated, mono-quaternized bipyridinium, which is pH dependent. The interesting properties from Poly($P\text{-}V\text{-}Me^{2+}$) and poly($P\text{-}V\text{-}H^{2+}$) stem from the behavior of the pendant viologen redox centers. The device based on poly($P\text{-}V\text{-}Me^{2+}$) has a narrow region (~200 mV) of gate voltage, V_G, where the source-drain current, I_D, is non-zero and has a sharp, pH-independent peak in the I_D-V_G plot at --0.53 V vs. SCE associated with the reversible, one-electron reduction of viologen. This result is consistent with electron self-exchange between redox centers being the mechanism for charge transport. The device based on poly($P\text{-}V\text{-}H^{2+}$) shows a pH-dependent I_D at fixed V_G, as expected from the electrochemical behavior from reversible protonation of the terminal N of the bipyridinium

group of poly(P-V-H^{2+}). The microelectrochemical transistor based on poly(P-V-H^{2+}) illustrates the design of chemically sensitive, molecule-based devices using conventional redox materials.

Introduction

In this article we report the synthesis and electrochemical properties of two redox polymers, poly(P-V-Me^{2+}), and poly(P-V-H^{2+}), derived from oxidative electropolymerization of (P-V-Me^{2+}), I, and (P-V-H^{2+}), II, equation (1). In recent years the development of new types

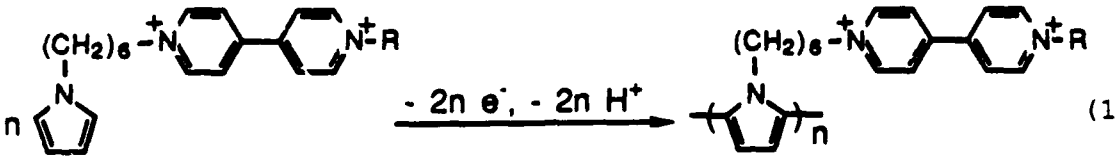

(1)

R = CH_3, I
H, II

of electroactive redox polymers has received considerable attention.[1] Polymers with conducting polymers such as poly(porrole) or poly(thiophene) as backbones and incorporating electroactive redox centers as pendant groups have been proven to be convenient materials for the preparation of polymer-modified electrodes containing a specific redox center.[2,3] Use of poly(P-V-Me^{2+}) and poly(P-V-H^{2+}) allows demonstration of the behavior of microelectrochemical transistors[4] based on the viologen redox center, (P-V-Me^{2+}), and a similar redox center, (P-V-H^{2+}), which is pH dependent, equation (2). The pH

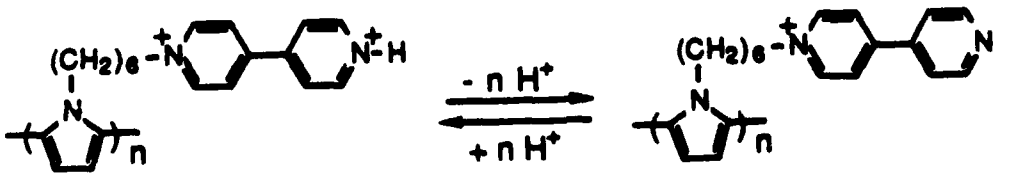

(2)

dependence of the electrochemical potential of poly(P-V-H^{2+}) is crucial to the demonstration of a pH-sensitive microelectrochemical transistor.[5] The acid-base reaction of interest is illustrated in equation (2).

Closely spaced (~1.5 μm) Au or Pt microelectrodes (~2.5 μm wide x 50 μm long x 0.1 μm high) have been used in the study of electroactive materials. Conducting polymers such as polypyrrole,[4] poly(N-methylpyrrole),[4b] polyaniline,[6] and poly(3-methylthiophene)[6b,7] have been used to modify pairs of microelectrodes to achieve molecule-based microelectrochemical devices which have functions analogous to solid-state transistors.[8] Conventional redox polymers are of interest because their optimal conductivity is confined to a narrow potential range, even though their absolute conductivity is relatively low in comparison to conducting polymers. Closely spaced microelectrodes derivatized with conventional redox materials such as viologen/quinone polymer,[9] ferrocyanide-loaded protonated poly(4-vinylpyridine),[10] and Prussian blue[11] have allowed the demonstration of microelectrochemical transistors based on conventional redox materials.

A microelectrochemical transistor based on a conventional redox material such as poly(P-V-Me^{2+}) is illustrated in Scheme I. Two closely spaced microelectrodes, in analogy to the source and drain of a solid-state transistor, are connected by a conventional

(a)

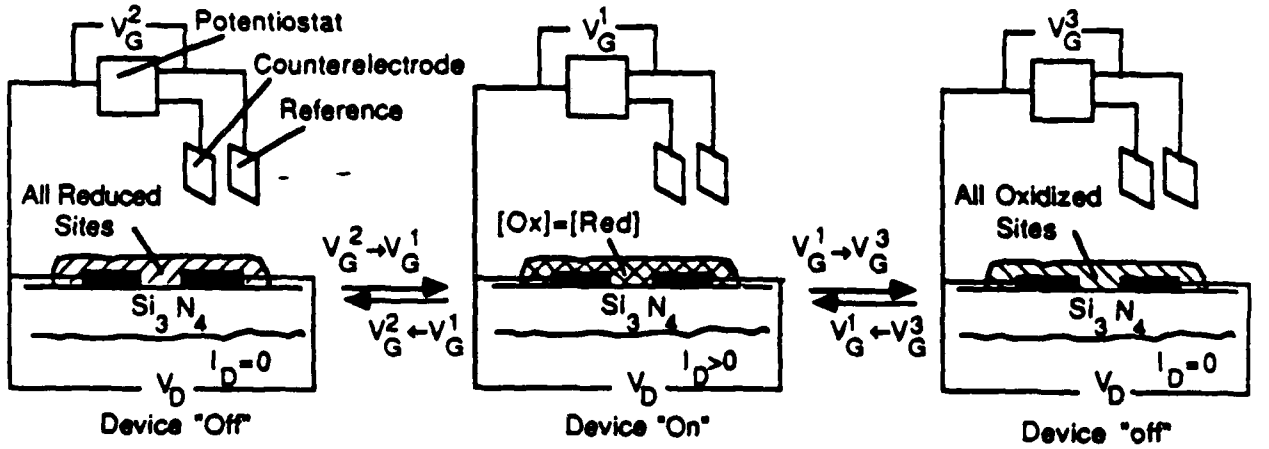

(b)

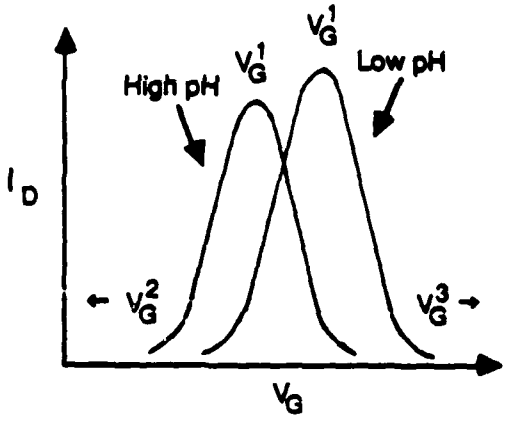

Scheme I. (a) A microelectrochemical transistor based on a conventional redox polymer operated at a small value of V_D. The device is only turned on to a significant extent at $V_G \approx E^{\circ\prime}$, V_G^1. At V_G significantly (>0.2 V) more negative ($V_G = V_G^2$) or positive ($V_G = V_G^3$) of $E^{\circ\prime}$ only the reduced or oxidized sites are present, respectively, and the device is off. (b) The I_D-V_G characteristic of a microelectrochemical transistor based on a redox polymer such as poly(P-V-H^{2+}) having a pH dependent $E^{\circ\prime}$.

redox polymer "channel". The essential property of the redox material is that its conductivity is a function of its state of charge, which can be controlled by the gate potential, V_G. Thus upon variation in V_G, there will be a change in the drain current, I_D, for a fixed potential between source and drain, V_D.

As shown in Scheme I, a microelectrochemical transistor based on a conventional redox polymer has an I_D-V_G characteristic with a sharp maximum in I_D at $V_G = E^{\circ\prime}$ of the redox polymer and a very narrow V_G region where $I_D > 0$. The characteristic arises because in a conventional redox polymer the mechanism of charge transport is electron self-exchange between adjacent oxidized and reduced sites.[12,13] The maximum "conductivity" of a conventional redox polymer is achieved when the polymer contains equal quantities of oxidized and reduced sites, which occurs when V_G is equal to $E^{\circ\prime}$ of the polymer.[12] When V_G is significantly negative or positive (~100 mV) of $E^{\circ\prime}$, all redox centers are in the reduced or oxidized state, respectively, and the conductivity is zero.

The exciting prospect associated with conventional redox polymer-based microelectrochemical transistors is that devices only turn on at particular values of V_G and, further, that the turn on value of V_G can be chemically dependent in a predictable manner. For a device based on poly(P-V-H^{2+}), the V_G required to turn on the device varies with pH, since the redox potential of poly(P-V-H^{2+}) is pH-

dependent. At a given V_G and V_D, a change in pH will cause a change in the ratio of oxidized to reduced redox centers, causing a change in I_D. The modification of microelectrodes with polymers, such as poly(P-V-H^{2+}), which have pH sensitive redox subunits, point with promise towards the fabrication of pH-sensitive microelectrochemicl transistors. It should be realized that poly(P-V-Me^{2+}) and poly(P-V-H^{2+}) represent polymers with interesting properties with respect to the poly(N-alkylpyrrole) backbone, but we have not elaborated these properties owing to the emphasis in the present work on the conventional redox centers which have a cnemically sensitive E°′. Transistors based on poly(N-alkylpyrrole) have been described elsewhere;[4b] here the N-alkylpyrrole merely provides a convenient precursor to a polymer containing the viologen redox centers.

There are several other pH-dependent microelectrochemical devices other than that described here. These include devices based on platinized poly(3-methylthiophene),[7b] a viologen/quinone polymer,[9] ferrocyanide-loaded protonated poly(4-vinylpyridine),[10] and electroactive metal oxides[14] (WO_3, NiO). The poly(P-V-H^{2+})-based microelectrochemical transistor is the first example of a pH-sensitive microelectrochemical device based on a redox polymer with a pH-dependent E°′. The concept of a three terminal device based on a polymer with a chemically dependent E°′ can be readily extended to develop a wide range of small, specific microelectrochemical sensors.

Experimental Section

Chemicals. CH_3CN was distilled from CaH_2 and stored under N_2. Tetrahydrofuran (THF) was dried by refluxing with Na/K and benzophenone until a characteristic blue color was evident, and the THF was then distilled under N_2. H_2O was Omnisolv HPLC grade. [n-Bu_4N]PF_6 was prepared by adding an aqueous solution of [n-Bu_4N]Br to an aqueous solution of NH_4PF_6 and collecting the precipitate followed by recrystallization from 95% EtOH and drying under vacuum at 100 °C overnight. n-BuBr, CH_3I, 4,4'-bipyridine, pyrrole, 6-chlorohexanol, p-toluenesulfonyl chloride, HPF_6, $K[Au(CN)_2]$ were commercially available and used as received.

Synthesis of 1-(n-butyl)-4,4'-bipyridinium bromide. A solution of n-BuBr (1.4 g) and 4,4-bipyridine (7.8 g) in 50 ml of CH_3CN was refluxed overnight. The mixture was then poured into Et_2O and the Br^- salt precipitated. The precipitated salt was collected and washed with Et_2O: yield, 2.05 g (71%); ^1H NMR (250 MHz, D_2O) δ 8.86 (d, 2 H), 8.65 (d, 2 H), 8.28 (d, 2 H), 7.79 (m, 2 H), 4.56 (t, 2 H), 1.93 (quintet, 2 H), 1.29 (m, 2 H), 0.85 (t, 3 H).

Synthesis of 1-(6-hydryxyl)-hexyl pyrrole.[15] A solution of pyrrole (8.5 g) in 20 ml of THF was slowly added to 20 ml of THF and 4.8 g of K in a three-necked flask. The solution was refluxed under N_2 until all the K was reacted. The resulting solution was cooled to room temperature and a solution of 6-chlorohexanol (8.2 g) in 20 ml of THF was slowly (to avoid excessive heating) added. After stirring

30 min, the solution was poured into 100 ml ice H_2O and extracted several times with 50 ml Et_2O. The Et_2O was dried over Na_2SO_4 and removed by rotary evaporation. The product was obtained by vacuum distillation: yield, 6.97 g (70%); bp 95 °C (0.025 torr); ^1H NMR (250 MHz, $CDCl_3$) δ 6.64 (t, 2 H), 6.13 (t, 2 H), 3.87 (t, 2 H), 3.60 (t, 2 H), 2.60 (s, 1 H), 1.76(m, 2 H), 1.54 (m, 2 H), 1.34 (m, 4 H).

Synthesis of 6-(pyrrol-1-yl)-hexyl p-toluenesulfonate.[16] A solution of 1-(6-hydryxyl)-hexyl pyrrole (0.84 g) and tosyl chloride (0.95 g) in 10 ml pyridine was stirred at 5 °C overnight. The mixture was poured into ice H_2O and extracted with Et_2O. The extract was washed with 5 % HCl(aq) and dried over Na_2SO_4. After removing the solvent, the desired tosylate was obtained as an orange solid: yield, 1.0 g (62 %); ^1H NMR (250 MHz, $CDCl_3$) δ 7.78 (d, 2 H), 7.34 (d, 2 H), 6.61 (t, 2 H), 6.13 (t, 2 H), 4.00 (t, 2 H), 3.83 (t, 2 H), 2.45 (s, 3 H), 1.68 (m, 4 H), 1.27 (m,4 H).

Synthesis of 1-(6-pyrrol-1-yl)-hexyl-4,4'-bipyridinium hexafluorophosphate ($P\text{-}V^+$). A solution of 6-(pyrrol-1-yl)-hexyl tosylate (1.6 g) and 4,4'-bipyridine (3.2 g) in 20 ml of CH_3CN was refluxed overnight. The solvent was reduced and a solid was precipitated after adding Et_2O. The tosylate salt was isolated from the unreacted 4,4'-bipyridine by filtration and converted to the PF_6^- salt by dissolving in H_2O and adding to a solution of 3g of NH_4PF_6 in 20 ml of H_2O. The PF_6^- salt precipitated and was recrystallized from EtOH: yield, 1.3 g (62%); ^1H NMR (250

MHz, CD_3COCD_3) δ 9.24 (d, 2 H), 8.85 (m, 2 H), 8.64 (d, 2 H), 7.97 (m, 2 H), 6.64 (t, 2 H), 5.94 (t, 2 H), 4.85 (t, 2 H), 3.88 (t, 2 H), 2.14 (m, 2 H), 1,74 (m, 2 H), 1.40 (m, 4 H); MS, M^+ 451.1624 (obsd), 451.1612 (calcd), composition $C_{20}H_{24}N_3PF_6$, $(M-PF_6)^+$ 306.1974 (obsd), 306.1970 (calcd), composition $C_{20}H_{24}N_3$.

Synthesis of 1-methyl-1'-(6-pyrrol-1-yl)-hexyl-4,4'-bipyridinium bishexafluorophosphate ($P\text{-}V\text{-}Me^{2+}$). A solution of ($P\text{-}V^+$) (0.9 g) and CH_3I (0.2 ml) in 30 ml of CH_3CN was refluxed overnight. The solvent was reduced and a solid precipitated after adding Et_2O. The I^- salt was converted to the PF_6^- salt by dissolving in H_2O and adding to a solution of 1 g of NH_4PF_6 in 10 ml of H_2O. The PF_6^- salt precipitated and was collected by filtration: yield, 0.74 g; ^1H NMR (250 MHz, CD_3COCD_3) δ 9.35 (m, 4 H), 8.79 (m, 4 H), 6.65(t, 2 H), 5.95(t, 2 H) 4.91(t, 2 H), 4.71 (s, 3 H), 3.88 (t, 2 H), 2.17 (m, 2 H), 1.77 (m, 2 H), 1.39 (m, 4 H); MS, $(M-PF_6)^+$ 466.1839 (obsd), 466.1847 (calcd), composition $C_{21}H_{27}N_3PF_6$, $(M-2PF_6)^+$ 321.2199 (obsd), 321.2205(calcd), composition $C_{21}H_{27}N_3$.

Synthesis of 1-H-1'-(6-pyrrol-1-yl)-hexyl-4,4'-bipyridinium bishexafluorophosphate ($P\text{-}V\text{-}H^{2+}$). To a solution of ($P\text{-}V^+$) (0.45 g) in 1 ml of CH_3CN at -40 °C was added a solution of HPF_6 (0.3 g, 60wt % solution in H_2O) in 1 ml of CH_3CN. The mixture was added to Et_2O and an oil appeared in the bottom of the flask. The oil was washed with Et_2O. A solid product was obtained after drying the oil in vacuo. ^1H NMR

(250 MHz, CD_3COCD_3) δ 9.83 (m, 4 H), 8.79 (m, 4 H), 6.65 (t, 2 H), 5.96 (t, 2 H), 4.93 (t, 2 H), 3.89 (t, 2 H), 2.17 (m, 2 H), 1.75 (m, 2 H), 1.40 (m, 4 H).

Electrochemical Equipment and Procedures. Electrochemical experiments were performed using either a PAR Model 363 potentiostat/galvanostat and Par Model 175 universal programmer with a Houston Instruments Model 2000 x-y recorder, or a Pine Instruments RDE-4 Bipotentiostat with a Kipp & Zonen BD 91 X-Y-Y' recorder. Absorption spectra were recorded on a HP 8451A Diode Array Spectrometer.

All electrochemical experiments were carried out under N_2 using a standard three electrode configuration with a Pt counter electrode and SCE or Ag^+/Ag (0.1 M $AgNO_3/CH_3CN$) as reference. The buffer solution was made of 0.1 M CH_3COOH and 0.01 M CH_3COONa aqueous solutions, and the pH was adjusted to the desired value by addition of concentrated NaOH or HCl solutions. Spectroelectrochemical measurements were made in a quartz cuvette with polymer-derivatized SnO_2 electrode as working electrode.

Preparation of Microelectrode Arrays. The microelectrode arrays used in the work consisted of eight, individually addressable Au microelectrodes each ~50 μm long, ~2.5 μm wide and ~0.1 μm high and separated from each other by ~1.5 μm. Fabrication and encapsulation of the microelectrode array has been described previously.[4b,17] Prior to use, microelectrodes were cleaned by an rf O_2 plasma etch followed by a negative potential excursion to give H_2

evolution. The microelectrodes were then tested by examining their electrochemical behavior in aqueous 0.1 M LiCl containing 5 mM $Ru(NH_3)_6^{3+}$. Good electrodes show a well-developed sigmoidal, current-voltage scan with a plateau current of 30 nA.

The Au microelectrodes were modified by electrochemical deposition of Au onto their surface to narrow the inter-electrode gap.[10,17b] The Au was deposited from aqueous 0.1 M K_2HPO_4 containing 70 mM $K[Au(CN)_2]$. The electrodes were plated one at a time by holding the one to be plated at a negative potential (--1.1 V) and all other electrodes not to plated at 0.1 V vs. SCE. As shown in Scheme II, electrodes #1, 3, 5, and 7 were plated with Au. The deposition of Au involved ~3 μC of charge per electrode plated and the inter-electrode gap was ~0.2 μm.

Electrode Derivatization. Poly(P-V-Me^{2+}) or poly(P-V-H^{2+}) can be grown onto electrode surfaces by oxidizing (P-V-Me^{2+}) or (P-V-H^{2+}) in CH_3CN/0.1 M [n-Bu_4N]PF_6 solution. The typical procedure involves cycling (100 mV/s) the potential of an electrode to be derivatized between 0.1 V and 1.4 V vs. SCE in the presence of 10 mM (P-V-Me^{2+}) or 40 mM (P-V-H^{2+}).

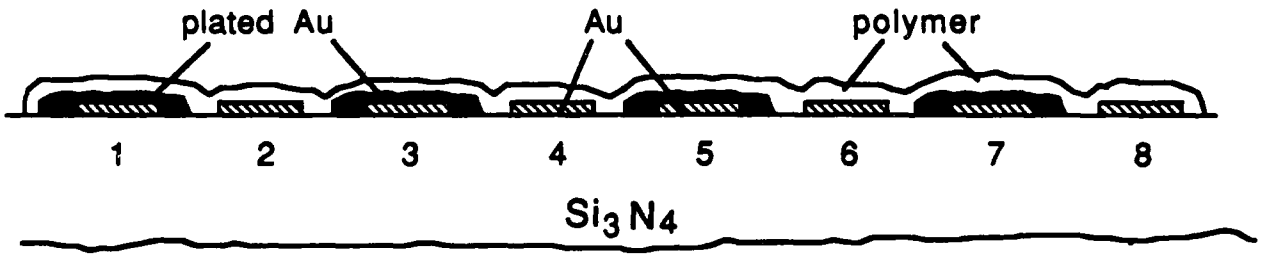

Scheme II. Arrangement of an array of Au microelectrodes used for experiments in this work.

Results and Discussion

Synthesis of Compounds ($P\text{-}V^{+}$), ($P\text{-}V\text{-}Me^{2+}$), ($P\text{-}V\text{-}H^{2+}$).

Compounds I and II were synthesized according to the methods detailed in the Experimental Section, Scheme III. The synthesis is straightforward and yields well-characterized molecules which can serve as precursors to polymers via oxidative polymerization, as developed below.

Electrochemistry of Compounds ($P\text{-}V^{+}$), ($P\text{-}V\text{-}Me^{2+}$), ($P\text{-}V\text{-}H^{2+}$).

The electrochemical behavior of ($P\text{-}V^{+}$), ($P\text{-}V\text{-}Me^{2+}$), and ($P\text{-}V\text{-}H^{2+}$) in CH_3CN/0.1 M [n-Bu_4N]PF_6 was investigated by cyclic voltammetry. Figure 1b shows the cyclic voltammogram of ($P\text{-}V^{+}$) in CH_3CN/0.1 M [n-Bu_4N]PF_6 revealing a reversible, one-electron wave at -0.96 V vs. SCE. The one-electron reduction reduction at -0.96 V vs. SCE is associated with the N-alkyl-4,4'-bipyridinium redox center. In addition there is a wave associated with the irreversible oxidation of the N-alkylpyrrolyl group at about 1.3 V vs. SCE, but the oxidation does not easily induce formation of a polymeric film. It seems that the uncoordinated pyridyl group prevents the polymerization of pyrrole. Similar results have been obtained in the cases of a N-substituted pyrrole bearing a bipyridyl group and a 3-substituted thiophene with a pyridyl group.[18]

Cyclic voltammetry of ($P\text{-}V\text{-}Me^{2+}$) in CH_3CN/0.1 M [n-Bu_4N]PF_6 reveals two reversible, one-electron waves associated with the viologen group with $E^{\circ\prime}$'s at -0.42 V and

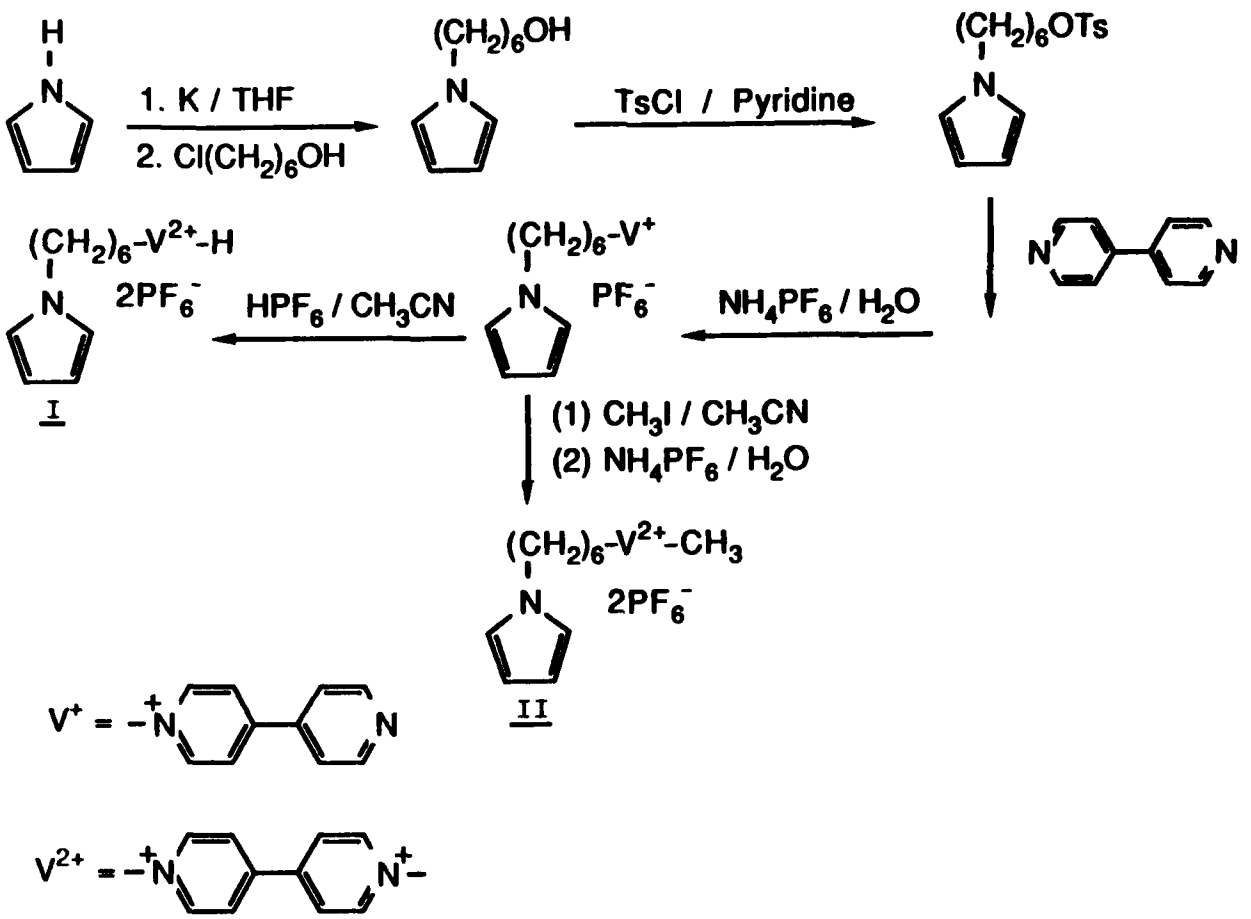

Scheme III. Synthetic procedure used to prepare compounds I and II. Details are given in the Experimental Section.

-0.84 V vs. SCE, as shown in Figure 1c. There is also an irreversible oxidation wave at ~1.3 V vs. SCE due to the oxidation of N-alkylpyrrole. With repeated potential scans of a Au electrode between 0.1 V and 1.4 V vs. SCE in a solution of 10 m$\underline{M}$ (P-V-Me^{2+}) in CH_3CN/0.1 $\underline{M}$ [$\underline{n}$-Bu_4N]PF_6, an oxidation wave grows at ~0.6 V vs. SCE. The wave at ~0.6 V vs. SCE is associated with the poly(N-alkylpyrrole). After polymer deposition, cyclic voltammetry of the derivatized electrode in the absence of (P-V-Me^{2+}) shows two reversible, one-electron waves at -0.38 V and -0.86 V associated with the pendant viologen redox centers and one reversible oxidation wave at 0.56 V vs. SCE associated with the oxidation of the poly(N-alkylpyrrole) backbone.[2a,4b,19] Using the viologen pendant group as an internal standard, the doping level of the oxidized poly(N-alkylpyrrole) backbone can be calculated. The ratio of the integrated waves associated with the viologen centers (0.0 to -1.2 V vs. SCE) and the poly(N-alkylpyrrole) redox system (0.0 to 1.0 V vs. SCE) is about 6.8 which indicates the oxidation of the poly(N-alkylpyrrole) chains to the extent of 1 charge per 3.4 pyrrole rings when the positive limit is +1.0 V vs. SCE. This level of "doping" is similar to that found by other workers.[2b,20]

The electrochemical behavior of (P-V-H^{2+}) in CH_3CN/0.1 $\underline{M}$ [$\underline{n}$-Bu_4N]PF_6 is very similar to that of (P-V-Me^{2+}) and very different from the non-protonated species (P-V^+). Compound (P-V-H^{2+}) has two reversible, one-electron reductions with

$E^{\circ\prime}$ at -0.41 V and -0.84 V vs. SCE, as shown in Figure 1a. The irreversible oxidation wave of the N-alkylpyrrole unit is at -1.3 V vs. SCE. Repeatedly scanning the potential of a Au electrode between 0.1 V and 1.4 V vs. SCE in a solution of 40 m<u>M</u> (P-V-H^2) in CH_3CN/0.1 <u>M</u> [<u>n</u>-Bu_4N]PF_6 results in the growth of a reversible oxidation wave at 0.53 V vs. SCE, associated with the deposited poly(N-alkylpyrrole). As shown in Figure 2, cyclic voltammetry of the modified electrode initially has two reduction waves at -0.40 V and -0.86 V vs. SCE, which correspond to the reduction of the protonated, mono-quaternized bipyridinium, but these are attenuated with time and finally disappear. Another reduction wave at -0.94 V vs. SCE, which is associated with the reduction of the mono-quaternized bipyridinium, simultaneously appears. The data show that deprotonation of poly(P-V-H^{2+}) occurs in the solvent/electrolyte used. The monoalkylated bipyridinium group of the polymer can be protonated again by dipping the electrode into a 1 <u>M</u> CF_3COOH/CH_3CN solution. Figure 3 illustrates the consequences of reversible deprotonation of poly(P-V-H^{2+}) on the electrochemical response of the polymer. Cyclic voltammetry of poly(P-V-H^{2+}) reveals a reversible wave at -0.52 V vs. SCE in pH 2 aqueous solution, associated with the protonated bipyridinium. In pH 6 aqueous solution, poly(P-V-H^{2+}) is deprotonated to form poly(P-V^+), which does not have a reduction wave at potentials more positive than

-0.7 V vs. SCE. After treating the modified electrode in 1 M CF_3COOH/CH_3CN, the wave corresponding to the reduction of the protonated form appears, as shown in Figure 3c. The polymer can be deprotonated again by dipping into 0.2 M pyridine/CH_3CN, and the wave at --0.9 V vs. SCE due to the reduction of poly(P-V^+) appears. Table I summarizes the E°'s for relevant solution and polymer-bound bipyridinium groups.

pH-Dependent Electrochemistry of Poly(P-V-H^{2+}) in Aqueous Solutions. The pH-dependence of the electrochemical behavior of a mono-quaternized bipyridinium salt, 1-(n-butyl)-4,4'-bipyridinium bromide, in aqueous solutions has been examined, Figure 4, as a model for the surface-confined polymer poly(P-V-H^{2+}). When the acidity of the aqueous solution is below pH 3, the cyclic voltammetry shows a reversible wave with E°' at -0.7 V vs. SCE which is near the first one-electron reduction potential of viologen and is largely pH-independent. When the acidity of the aqueous solution is between pH 4 and pH 6, the potential of the reversible reduction shifts to negative potentials with increase in pH. As shown in Figure 5, the slope of the E°' vs. pH plot is -57 mV, consistent with the electrode process being a 1 H^+/1 e^- reaction. When the acidity of the solution is above pH 7, the cyclic voltammetry becomes complicated due to the overlap of the first reduction wave of the deprotonated species and the second reduction wave of

the protonated species and the adsorption of reduced species on the electrode. The electrochemical behavior is consistent with the reversible protonation illustrated in equation (3). In acid solution the electrochemistry is

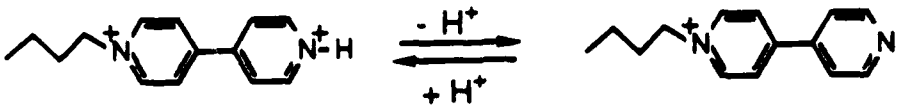

(3)

quite similar to that for a simple viologen, but the system shows a strong pH dependence in the range pH 3 to 6.

The poly(P-V-H^{2+}) film is electroactive in an aqueous solution, and the electrochemical behavior of the 4,4′-bipyridinium pendant groups of this polymer is similar to that of 1-(n-butyl)-4,4′-bipyridinium in solution. The pH-dependence of the cyclic voltammetry for poly(P-V-H^{2+}) is shown in Figure 6 for two coverages. When the pH is below 2, the redox wave has a potential that is pH-independent. When the pH is above 2, the redox wave is pH-dependent and shifts to negative potentials with increasing pH. The slope of $E^{\circ\prime}$ vs. pH plot is about -58 mV, as shown in Figure 5. This result indicates that the overall electrode reaction is a 1 H^+/1 e^- process as found for the solution species. For the poly(P-V-H^{2+}) of $\Gamma = 5 \times 10^{-10}$ mol/cm^2, corresponding to ca. 5 monolayers based on a monolayer coverage of ~10^{-10} mol/cm^2, the cyclic voltammetry is analogous to that obtained for the solution redox species; that is, the cathodic and anodic peak currents are independent of pH. For the thicker film of Γ ~10^{-8} mol/cm^2, corresponding to

ca. 100 monolayers, the peak currents decrease with increasing pH. The results are associated with the fact that a proton addition-elimination reaction is involved in the overall electrode reaction of the poly(P-V-H^{2+}) film. When the coverage is low, proton transfer between solution and polymer is very rapid and a decrease in proton concentration will not affect the apparent rate of the overall electrode reaction. When the coverage of the polymer film is high, proton transfer between solution and polymer becomes sluggish. The magnitude of the peak current reflects the apparent rate of the overall electrode reaction which decreases with a decrease in the concentration of proton. Similar behavior has also been observed for other surface-confined redox polymers.[21] Another feature that needs to be noted is that the pK_a of the polymer-bound mono-quaternized bipyridinium is smaller than that of the monomer, as shown in Figure 5. This shift in pK_a for solution vs. surface-bound species is similar to the shift reported for poly(ethyleneimine)-bound N-alkyl-4,4'-bipyridinium.[22]

Spectroelectrochemistry of Poly(P-V-Me^{2+}) and Poly(P-V-H^{2+}). Spectroelectrochemical studies were carried out in order to obtain additional data establishing the similarity of poly(P-V-Me^{2+}) and poly(P-V-H^{2+}) films. Figure 7 shows the UV-Vis absorption spectra of an SnO_2 electrode derivatized with poly(P-V-Me^{2+}) in pH 2 and pH 7 buffer solutions with

electrode potentials at 0.0 V and -0.8 V vs. SCE. The species having absorption bands at ~364 nm and 542 nm is associated with the one-electron reduction of the pendant viologen redox centers of poly(P-V-Me^{2+}). Essentially the same absorption has been observed for other reduced viologen-based redox polymers.[23] This result is consistent with the lack of interaction between the polypyrrole backbone and the viologen pendant groups in poly(P-V-H^{2+}). The absorption spectra are insensitive to pH as expected from the pH-independent electrochemistry of viologen-based polymers.[23]

The UV-Vis absorption spectra of a SnO_2 electrode derivatized with poly(P-V-H^{2+}) in pH 2 buffer solution for electrode potentials of 0.0 V and -0.8 V vs. SCE are shown in Figure 7a. The reduced form of poly(P-V-H^{2+}) has absorption similar to that of reduced viologen, with absorption maxima at ~362 nm and 534nm. The spectral similarity to reduced poly(P-V-Me^{2+}) indicates that reduction of the protonated, mono-quaternized bipyridinium is analogous to that of viologen and the structures of the reduced products are similar to one another. The point is that the protonated N-alkyl-4,4'-bipyridinium species behaved essentially as an N,N'-dialkyl-4,4'-bipyridinium with respect to electrochemical and optical properties. At pH 7 all mono-quaternized bipyridinium groups of poly(P-V-H^{2+}) are in the deprotonated form, and there is no reduction wave appearing at a potential more positive than -0.8 V vs.

SCE. Thus, changing the potential of a poly(P-V-H^{2+})-coated electrode from 0.0 V to -0.8 V vs. SCE does not cause any change in its UV-Vis absorption. The spectroelectrochemical behavior of poly(P-V^{+}) in non-aqueous media has not been investigated.

Charge Transport from One Microelectrode to Another via Pendant Viologen Redox Centers. Charge transport properties of the viologen redox centers of poly(P-V-Me^{2+}) have been investigated by steady-state experiments. An array of eight microelectrodes each initially ~50 μm long x 2.5 μm wide x 0.1 μm high and separated from each other by ~1.5 μm are first electrochemically plated with Au to close the gap to ~0.2 μm, Scheme II. The microelectrode array is then derivatized with poly(P-V-Me^{2+}) to "connect" the microelectrodes with the polymer. The poly(P-V-Me^{2+}) film is formed by electropolymerization of (P-V-Me^{2+}) in CH_3CN/0.1M [n-Bu_4N]PF_6 in the same manner as that used to derivatize conventional macroscopic electrodes.

The steady-state charge transport via the viologen centers of poly(P-V-Me^{2+}) in CH_3CN/0.1 M [n-Bu_4N]PF_6 has been studied using a microelectrode array like that sketched in Scheme II. Microelectrodes #2, 4, 6, and 8 are used as the "generator" and microelectrodes #1, 3, 5, and 7 are used as the "collector". The potential of the collector electrodes is held at 0.0 V vs. Ag^{+}/Ag, and the currents at the generator and at the collector are monitored upon

scanning the potential of the generator from 0.0 V to -0.9 V vs. Ag^+/Ag. This methodology resembles a ring-disk electrochemical experiment where the generator is the disk and the collector is the ring. Such experimentation has recently been reported for microelectrode arrays coated with polyvinylferrocene,[17] a viologen/quinone polymer,[9] or ferrocyanide-loaded, protonated poly(4-vinylpyridine).[10]

Figure 8 illustrates typical data for steady-state charge transport properties of a poly(P-V-Me^{2+})-coated microelectrode array. The data show that there is a steady-state current between the poly(P-V-Me^{2+})-connected microelectrodes when the potential of the generator is moved to a potential where the viologen groups of the polymer begin to be reduced. The steady-state current reaches a plateau when the generator potential is approximately -0.8 V vs. Ag^+/Ag where the viologen, V^{2+}, groups near the generator are fully reduced to V^+ and the collector is held at 0.0 V vs Ag^+/Ag where the viologen centers are in the V^{2+} state. Under such conditions, $[V^{2+}] = 0$ at the generator and $[V^+] = 0$ at the collector, the largest possible concentration gradient exists, giving the maximum current through the polymer. Increasing the voltage difference by moving the generator more negative does not increase the steady-state current because the concentration gradient does not increase appreciably. It is noted that the $E_{1/2}$ for half-maximum current is at $E^{o\prime}(V^{2+/+})$ where $[V^+]$ at the generator is half of the sum of $[V^{2+}]$ and $[V^+]$.

Qualitatively, these features are analogous to those observed with other redox polymers in sandwich electrodes,[12] where the redox conduction is treated as concentration-gradient-driven electron diffusion.

Figure 8 also presents the temperature dependence of the steady-state charge transport for viologen redox centers of poly(P-V-Me^{2+}) showing that the current for the steady-state charge transport increases significantly for increasing temperature. Charge transport in redox polymers can be treated as a thermally activated diffusion process.[24] A plot of logarithm of the limiting current vs. 1/T is linear as shown in the inset of Figure 8. The slope of the straight line gives an Arrhenius activation energy for electron diffusion of 10.2 kcal/mol, which is slightly larger than the value of 8.9 kcal/mol reported for another viologen-based polymer[25] and is similar to the the value of 9.8 kcal/mol for polythiophene-bound viologen.[3]

The charge transport properties of poly(P-V-Me^{2+}) in aqueous solution have also been studied using the generator and collector technique. Figure 9 presents data for steady-state charge transport properties of a poly(P-V-Me^{2+})-modified microelectrode array in pH 3 and pH 6 buffer solutions. The generator/collector current-voltage curves measured in aqueous solution are similar to those measured in CH_3CN. It must pointed out that the same current-potential relationship and the same magnitude of the plateau

current holds at different pH's, as expected from the pH-independent reduction of the viologen group.[23]

A redox polymer-coated microelectrode array has been demonstrated to be a device useful for measuring the diffusion coefficient for charge transport, D_{CT}, for the polymer.[10,11a] Using the previously reported method,[11a] we estimate D_{CT} to be ~1.1 x 10^{-9} cm^2/s for charge transport via the viologen, $V^{2+/+}$, system of poly(P-V-Me^{2+}) at 298 K in CH_3CN/0.1 M $[n\text{-}Bu_4N]PF_6$, somewhat below the value found for a similar polymer based on a poly(3-alkylthiophene).[3] The lower value of D_{CT} might be due to the use of the hexyl chain rather than a propyl chain as in the polythiophene case.[3] The D_{CT} for the poly(P-V-Me^{2+}) is not exceptional; the value is large enough to conveniently measure steady-state currents.

Poly(P-V-Me^{2+})-based Microelectrochemical Transistor.

Figure 10 illustrates the steady-state electrical characteristics of a poly(P-V-Me^{2+})-based microelectrochemical transistor in the region where the turn on is associated with the $V^{2+/+}$ redox system. The microelectrode array used is like that shown in Scheme II where the Au microelectrodes #2, 4, 6, and 8 are regarded as the "source" and the microelectrodes #1, 3, 5, and 7 are regarded as the "drain" of the transistor. The wiring for the transistor is as in Scheme I. In accord with a concentration gradient driven, self-exchange charge

transport mechanism, a microelectrochemical transistor based on conventional redox polymers shows only a narrow region of V_G where the device is "on" and a sharp maximum in I_D at V_G = $E^{\circ\prime}$ of the redox polymer. Figure 10 shows the I_D-V_G characteristic to depend on V_D. There is a sharp (90 mV width at half-height when V_D = 40 mV) peak in the I_D-V_G plot at --0.53 V vs. SCE associated with the reversible, one-electron reduction of the viologen centers, and the position and the height of the peak is pH-independent. The second important feature of Figure 10 is that the height and width of the peak become greater for larger V_D. Whenever V_D exceeds 0.3 V the maximum I_D does not increase, because the maximum gradient in concentration of the V^{2+} and V^{+} is no longer influenced by V_G. The third significant feature of Figure 10 is that the region of V_G where $I_D > 0$ is very narrow, being about 200 mV. For V_G > 100 mV away from $E^{\circ\prime}(V^{2+/+})$, I_D approaches zero, because the self-exchange mechanism for charge transport requires significant concentrations of both reduced and oxidized centers.

The poly(N-alkylpyrrole) backbone has no relevance to the conduction of the device for the following reasons. First, the $E^{\circ\prime}$ value for the viologen redox center is negative of the potential where the poly(N-alkylpyrrole) is oxidized and becomes significantly conducting.[4b,18] Second, in contrast to a conducting polymer-based microelectrochemical transistor which shows a broad region of V_G where the device is on,[4b,7] the poly(P-V-Me^{2+})-based

device shows only a narrow region of V_G where the device is on. Accordingly, the I_D-V_G characteristics for the poly(P-V-Me^{2+})-based transistor is consistent with expectations for conventional redox conduction. The poly(P-V-Me^{2+})-based device shows turn on for positive V_G's, but the characteristics are unexceptional compared to poly(N-methylpyrrole)-based devices.[4b]

pH-Dependent Charge Transport of Poly(P-V-H^{2+}). A microelectrochemical transistor based on poly(P-V-Me^{2+}) is insensitive to pH because the electrochemical behavior of the viologen centers in poly(P-V-Me^{2+}) is pH-independent. However, for a conventional redox polymer-based microelectrochemical transistor, $I_{D(max)}$ occurs at E°', and the value of I_D at fixed V_G and V_D will depend on the chemical environment whenever the redox material has a chemically dependent E°'. It should be possible to make a pH-sensitive microelectrochemical transistor based on poly(P-V-H^{2+}) , since this polymer has a pH-dependent E°', Figure 5 and 6.

The charge transport properties of poly(P-V-H^{2+}) have been studied with a poly(P-V-H^{2+})-derivatized microelectrode array using the generator/collector method as discussed above. Figure 11 illustrates data for the steady-state charge transport properties of a poly(P-V-H^{2+})-coated microelectrode array in aqueous solutions of differing pH. At constant pH, the generator/ collector current-voltage

curves for poly(P-V-H^{2+}) are analogous to those for poly(P-V-Me^{2+}), with half-maximum steady-state collector current when the generator is at $E^{o\prime}$ and maximum steady-state current at generator potential significantly negative of $E^{o\prime}$. However, at significantly negative potentials, current due to hydrogen evolution occurs at the generator. Upon variation of pH, it is observed that the potential of the half-maximum steady-state current is pH-dependent and shifts negative with increase in pH. Moreover, the magnitude of the pH-dependent potential shift is in accord with the data shown in Figure 5. These results are consistent with the expectation that the overall electrode reduction of poly(P-V-H^{2+}) involves 1 H^+ and 1 e^- per bipyridinium center. The magnitude of the plateau current also depends on pH with higher pH's giving less current. Because the coverage of poly(P-V-H^{2+}) on the microelectrode array is high ~3 x 10^{-8} mol/cm^{-2}, proton transfer within the polymer and between solution and polymer is slow. A proton addition-elimination reaction to the bipyridinium group may control the rate of charge transfer when the concentration of protons in the solution is low, and the steady-state current would decrease with a decrease in the concentration of protons.

pH-Sensitive Microelectrochemical Transistor. The data in Figure 11 indicate that variation in I_D should be observed upon variation of pH in a solution in contact with a poly(P-V-H^{2+})-based transistor at fixed V_G and V_D. Using poly(P-V-

H^{2+}) as the active material in a microelectrochemical transistor allows demonstration of a pH-sensitive, molecule-based device that turns on or off by changing the concentration of protons in solution. Figure 12 illustrates variation of I_D from pH variation at fixed V_G and V_D for a microelectrochemical transistor based on poly(P-V-H^{2+}). The microelectrode array used is like that shown in Scheme II, where microelectrodes #2, 4, 6, and 8 are regarded as the "source" and microelectrodes #1, 3, 5, and 7 are regarded as the "drain" of the transistor. The device is on at pH = 3 for V_G = -0.4 V vs. SCE and V_D = 200 mV. Upon changing the pH of the solution from pH 3 to pH 6, the device is turned from on to off. Because the reduction potential of the protonated mono-quaternized bipyridinium is pH dependent, the increase in pH causes a change in the redox potential. At pH 6, the $E^{\circ\prime}$ of this polymer is -0.72 V vs. SCE. All the redox sites of poly(P-V-H^{2+}) are in the oxidized form when V_G = -0.4 V vs. SCE and charge transfer is blocked. There is no current flow between source and drain. These results are consistent with the expectations of redox conduction and the pH-dependent electrochemical behavior of poly(P-V-H^{2+}).

Conclusions

The poly(P-V-Me^{2+})-based transistor allows the demonstration of the characteristics of a microelectrochemical transistor based on a conventional redox polymer as the "channel". The conventional redox polymer endows the device with a unique I_D-V_G characteristic: a narrow range of V_G (~200 mV) where $I_D > 0$ with a sharp, pH-independent I_D peak at $V_G = E^{\circ\prime}$ of the redox polymer. The specific region where the device is on is an intrinsic characteristic that should be useful in sensor applications.

Cyclic voltammetry and spectroelectrochemical studies of poly(P-V-H^{2+}) show that the reduction of this polymer in aqueous solution involves 1 H^+ and 1 e^- per bipyridinium center and the redox potential is pH dependent. The effect of pH on the behavior of poly(P-V-H^{2+})-based microelectrochemical transistors has been probed, and the results are in accord with the pH dependence of the electrochemical reduction of poly(P-V-H^{2+}) and with the characteristics of devices based on conventional redox materials. Although the microelectrochemical devices based on conventional redox polymers have low conductivity compared to devices based on conducting polymers, unique opportunities are presented by the remarkable range of intrinsic chemical specificity of redox polymers with respect to variation in $E^{\circ\prime}$ of the redox system.

The poly(P-V-H^{2+})-based, pH-sensitive microelectrochemical transistor illustrates the prescription for designing a chemically sensitive device: find a reversible redox active molecule with the desired chemical effect on $E^{\circ\prime}$ and incorporate it into a polymer, and then apply the polymer to microelectrode arrays.

Acknowledgments. We thank the Office of Naval Research and the Defense Advanced Research Projects Agency for partial support of this research.

References

1. (a) Murray, R. W. in "Electroanalytical Chemistry", Vol. 13, Bard, A. J. ed., Marcel Dekker, New York, 1984, p. 191. (b) Wrighton, M. S. Science, 1986, 231, 32.

2. (a) Bidan, G.; Deronzier, A.; Moutet, J. C. J. Chem. Soc. Chem. Commun., 1984, 1185. (b) Coche, L.; Deronzier, A.; Moutet, J. C. J. Electroanal. Chem., 1986, 198, 187. (c) Coche, L.; Moutet, J. C. J. Electroanal. Chem., 1987, 224, 111. (d) Coche, L.; Moutet, J. C. J. Am. Chem. Soc., 1987, 109, 6887. (e) Bidan, G.; Deronzier A.; Moutet J. C. Nouv. J. Chim., 1984, 8, 501. (f) Eaves, J. G.; Munro, H. S.; Parker, D. Inorg. Chem., 1987, 26, 644. (g) Haimerl, A.; Merz, A. Angrew. Chem. Int. Ed. Engl., 1986, 25, 180. (h) Audebert, P.; Bidan, G.; Lapkowski, M. J. Chem. Soc. Chem. Commun., 1986, 887.

3. Shu, C. F.; Wrighton, M. S. submitted for publication.

4. (a) White, H. S.; Kitllesen, G. P.; Wrighton, M. S. J. Am. Chem. Soc., 1984, 106, 5357. (b) Kittlesen, G. P.; White, H. S.; Wrighton, M. S. J. Am. Chem. Soc., 1984, 106, 7389.

5. Wrighton, M. S.; Thackeray, J. W.; Natan, M. J.; Smith, D. K.; Lane, G. A.; Belanger, D. Phil. Trans. Royal Soc. Lond., 1987, B316, 13.

6. (a) Paul, E. W.; Ricco, A. T.; Wrighton, M. S. J. Phys. Chem., 1985, 89, 1441. (b) Lofton, E. P.; Thackeray, J. W.; Wrighton, M. S. J. Phys. Chem., 1986, 90, 6080.

7. (a) Thackeray, J. W.; White, H. S.; Wrighton, M. S. J. Phys. Chem., 1985, 89, 5133. (b) Thackeray, J. W.; Wrighton, M. S. J. Phys. Chem., 1986, 90, 6674.

8. Sze, S. M. Physics of Semiconductor Devices; Wiley: New York, 1981.

9. (a) Smith, D. K.; Lane, G. A.; Wrighton, M. S. J. Am. Chem. Soc., 1986, 108, 3522. (b) Smith, D. K.; Lane, G. A.; Wrighton, M. S. submitted.

10. Belanger, D.; Wrighton, M. S. Anal. Chem., 1987, 59, 1426.

11. (a) Chidsey, C. E.; Feldman, B. J.; Lundgren, C.; Murray, R. W. Anal. Chem., 1986, 58, 601. (b) Belanger, D.; Wrighton, M. S. unpublished results.

12. (a) Pickup, P. G.; Murray, W. R. J. Am. Chem. Soc., 1983, 105, 4510. (b) Pickup, P. G.; Kutner, W.; Leidner, C. R.; Murray, R. W. J. Am. Chem. Soc., 1984, 106, 1991. (c) Pickup, P. G.; Murray, R. W. J. Electrochem. Soc., 1984, 131, 833.

13. Kaufman, F. B.; Engler, E. M. J. Am. Chem. Soc., 1979, 101, 547.

14. (a) Natan, M. J.; Mallouk, T. E.; Wrighton, M. S. J. Phys. Chem., 1987, 91, 648. (b) Natan, M. J.; Belanger, D.; Carpenter, M. S.; Wrighton, M. S. J. Phys. Chem., 1987, 91, 1834.

15. Bidan, G. Tetrahedron Lett., 1985, 26, 735.

16. Marvel, C. S.; Sekera, V. C. Org. Synth., Coll. Vol. 3, 366.

17. (a) Kittlesen, G. P.; White, H. S.; Wrighton, M. S. J. Am. Chem. Soc., 1985, 107, 7373. (b) Kittlesen, G. P. Ph.D. Thesis, Massachusetts Institute of Technology, 1985.

18. (a) Daire, F.; Bedioui, F.; Devynck, J.; Bied-Charreton, C. J. Electroanal. Chem., 1986, 205, 309. (b)Bauerle, P.; Wrighton, M. S. unpublished result.

19. (a) Diaz, A. F.; Castillo, J.; Logan, J. A.; Lee, W. Y. J. Electroanal. Chem., 1981, 129, 115. (b) Diaz, A. F.; Castillo, J.; Kanazawa, K. K.; Logan, J. A.; Salmon, M.; Fajardo, O. J. Electroanal. Chem., 1982, 133, 233.

20. Kanazawa, K. K.; Diaz, A. F.; Gill, W. D.; Grant, P. M.; Street, G. B.; Gradini, G. P.; Kwak, J. F. Synth. Met., 1979/80, 1, 329.

21. (a) Oyama, N.; Hirabayashi, K.; Ohsaka, T. Bull. Chem. Soc. Jpn., 1986, 59, 2071. (b) Oyama, N.; Hirokawa, T.; Yamaguchi, S.; Ushizawa, N.; Shimomura, T. Anal. Chem., 1987, 59, 258.

22. O'Connell, K. M.; Waldner, E.; Roullier, L.; Laviron, E. J. Electroanal. Chem., 1984, 162, 77.

23. Bookbinder, D. C.; Wrighton, M. S. J. Electrochem. Soc., 1983, 130, 1080.

24. (a) Daum, P.; Lenhard, J. R.; Rolison, D.; Murray, R. W. J. Am. Chem. Soc., 1980, 102, 4649. (b) Oyama, N.; Anson, F. C. J. Electrochem. Soc., 1980, 127, 640.

25. (a) Lewis, T. J.; White, H. S.; Wrighton, M. S. J. Am. Chem. Soc., 1984, 106, 6947. (b) Lewis, T. J. Ph.D. Thesis, Massachusetts Institute of Technology, 1984.

Table I. Formal Potentials for Relevant Species.[a]

Species	Solvent	E°′, V vs. SCE
$(P\text{-}V^{+/0})$	CH_3CN	-0.96
$(P\text{-}V\text{-}Me^{2+/+/0})$	CH3CN	-0.42, -0.84
$(P\text{-}V\text{-}H^{2+/+/0})$	CH_3CN	-0.41, -0.84
$(\underline{n}\text{-}Bu\text{-}V^{+})$[b]	H_2O/pH = 3	-0.70
poly$(P\text{-}V\text{-}Me^{2+/+/0})$	CH_3CN	-0.38, -0.86
poly$(P\text{-}V\text{-}Me^{2+/+})$	H_2O/pH = 2-7	-0.53
poly$(P\text{-}V\text{-}H^{2+/+/0})$	CH_3CN	-0.40, -0.86
poly$(P\text{-}V\text{-}H^{2+/+})$	H_2O/pH = 3	-0.55
poly$(P\text{-}V^{+/0})$	CH_3CN	-0.94

[a] Data are for the reversible, one-electron redox systems associated with the 4,4′-bipyridinium redox centers in solution or for surface-confined polymers.

[b] $(\underline{n}\text{-}Bu\text{-}V^{+})$ ≡ N-(n-butyl)-4,4′-bipyridinium.

Figure Captions.

Figure 1. Cyclic voltammetry as a function of sweep rate for (a) (P-V-H^{2+}), (b) (P-V^{+}), (c) (P-V-Me^{2+}), in CH_3CN/0.1 M [n-Bu_4N]PF_6.

Figure 2. Cyclic voltammetry of a poly(P-V-H^{2+})-modified Au electrode repeatedly scanned (200 mV/s) between 0.0 V and -1.3 V vs. Ag^{+}/Ag in CH_3CN/0.1 M [n-Bu_4N]PF_6.

Figure 3. Cyclic voltammetry of an electrode derivatized with poly(P-V-H^{2+}) and its deprotonated form in various solutions. Scan rate: 100 mV/s.

Figure 4. Cyclic voltammetry of 1-(n-butyl)-4,4'-bipyridinium bromide in 0.1 M KCl aqueous solution of various pH's. Scan rate: 100 mV/S.

Figure 5. Variation of redox potential with pH for 1-(n-butyl)-4,4'-bipyridinium (•) and poly(P-V-H^{2+}) (o).

Figure 6. Cyclic voltammetry of poly(P-V-H^{2+}) films on SnO_2 electrodes in 0.1 M $LiClO_4$ aqueous solutions of various pH's (a) at low coverage (~5 x 10^{-10} mol/cm^2), scan rate: 70 mV/s; (b) at high coverage (~10^{-8} mol/cm^2), scan rate: 3 mV/s.

Figure 7. UV-Vis absorption spectra of optically transparent SnO_2 electrodes derivatized with polymer at 0.0 V (oxidized) and -0.8 V (reduced) vs. SCE in 0.1 M $LiClO_4$(aq) (a) Poly(P-V-H^{2+}), at pH 2; (b) poly(P-V-Me^{2+}), at pH 2; (c) poly(P-V-Me^{2+}), at pH 7.

Figure 8. Generation/collection cyclic voltammetry as a function of temperature at an interdigitated array of microelectrodes derivatized with poly(P-V-Me^{2+}) in CH_3CN/0.1 M [n-Bu_4N]PF_6. The potential of generator electrodes is scanned at 10 mV/s while the potential of collector electrodes is held at 0.0 V vs. Ag^+/Ag. Inset: Arrhenius plot; logarithm of the steady-state current vs. 1/T.

Figure 9. Generation/collection cyclic voltammetry of an interdigitated array of microelectrodes coated with poly(P-V-Me^{2+}) in 0.1 M $LiClO_4$(aq) at pH 6 and 3. The potential of generator electrodes is scanned at 2 mV/s while the potential of collector electrodes is held at 0.0 V vs. SCE.

Figure 10. Drain current, I_D, vs. gate voltage, V_G, for various drain voltages, V_D (40, 60, 80 mV) of a poly(P-V-Me^{2+})-based microelectrochemical transistor in H_2O/0.1 M $LiClO_4$. The gate voltage is scanned at 0.5 mV/s. The electrochemical circuitry used in this experiment is that of Scheme I.

Figure 11. Generation/collection cyclic voltammetry of an interdigitated array of microelectrodes modified with poly(P-V-H^{2+}) in 0.1 M $LiClO_4$(aq) of various pH's. The potential of generator electrodes is scanned at 1 mV/s while the potential of collector electrodes is held at 0.0 V vs. SCE.

Figure 12. I_D vs. time for poly(P-V-H^{2+})-based microelectrochemical transistor upon variation of pH, V_G = -0.4 V vs. SCE, V_D = 200 mV.

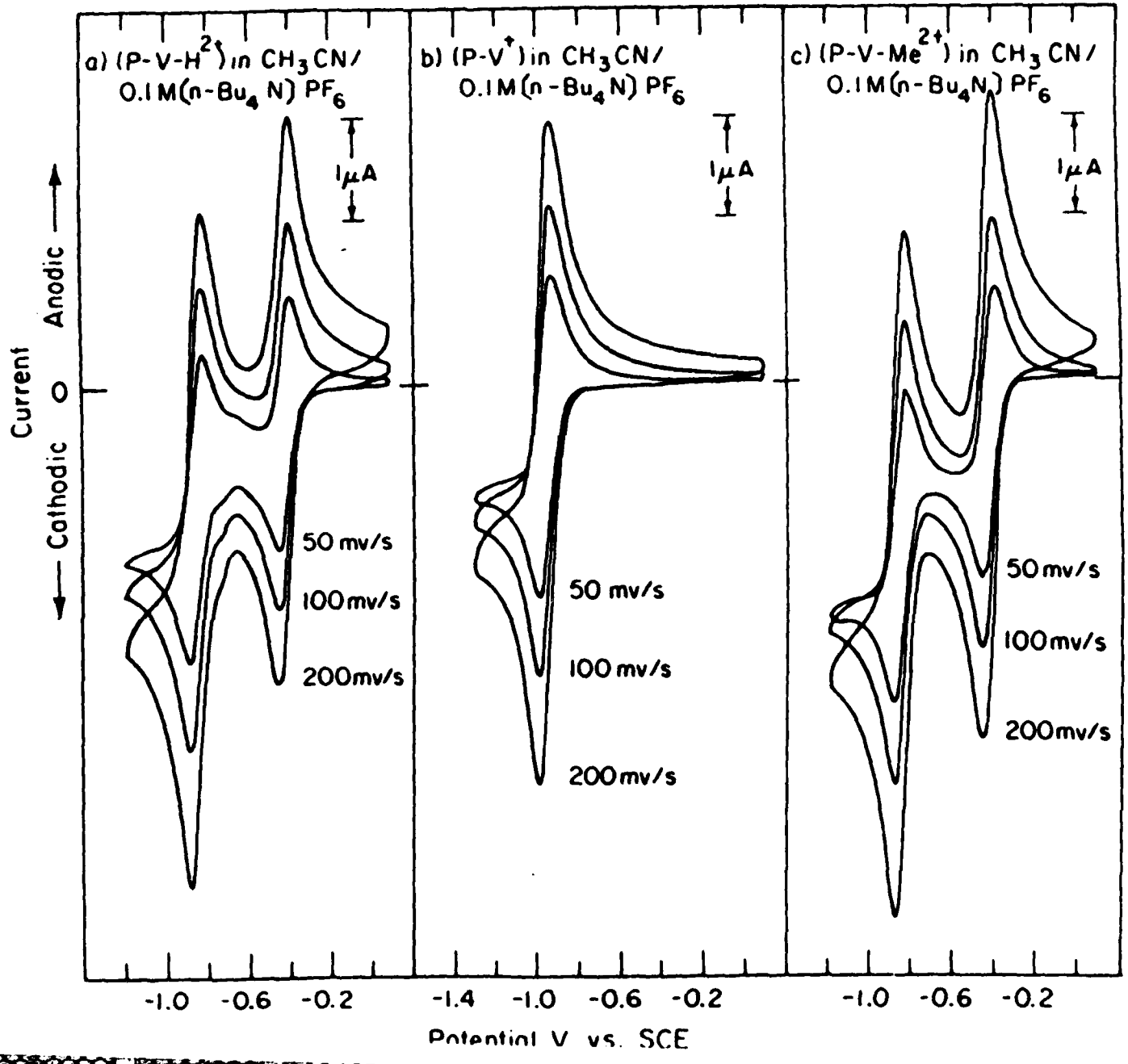
a) (P-V-H2+) in CH3CN/ 0.1M(n-Bu4N) PF6
b) (P-V+) in CH3CN/ 0.1M(n-Bu4N) PF6
c) (P-V-Me2+) in CH3CN/ 0.1M(n-Bu4N) PF6
1μA
Current
Anodic
0
Cathodic
50 mv/s
100 mv/s
200 mv/s
-1.0 -0.6 -0.2
-1.4 -1.0 -0.6 -0.2
Potential V vs. SCE

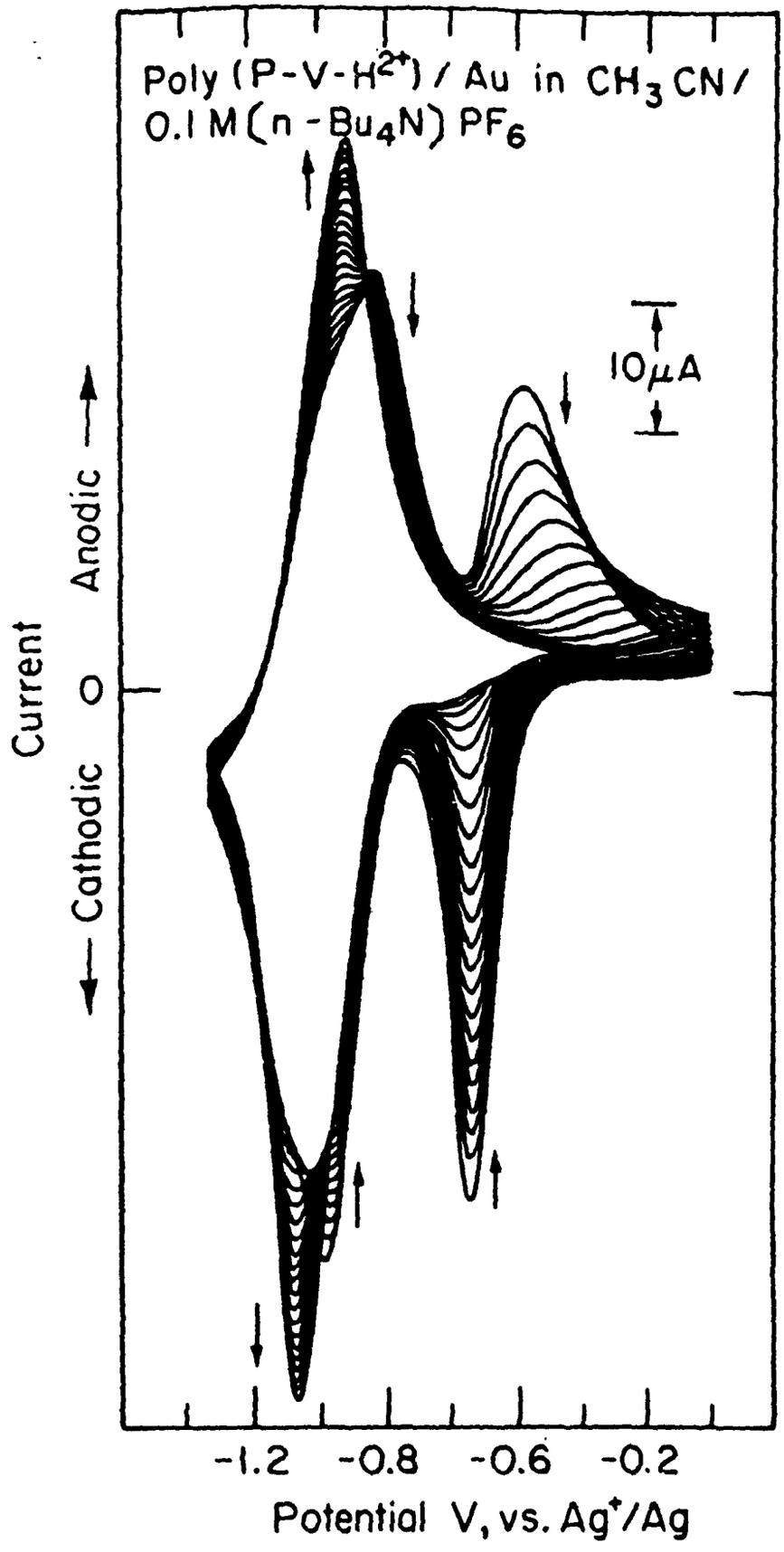
Poly (P-V-H^{2+}) / Au in CH_3CN /
0.1 M (n-Bu_4N) PF_6
10 μA
Current
Anodic
O
Cathodic
-1.2
-0.8
-0.6
-0.2
Potential V, vs. Ag^+/Ag

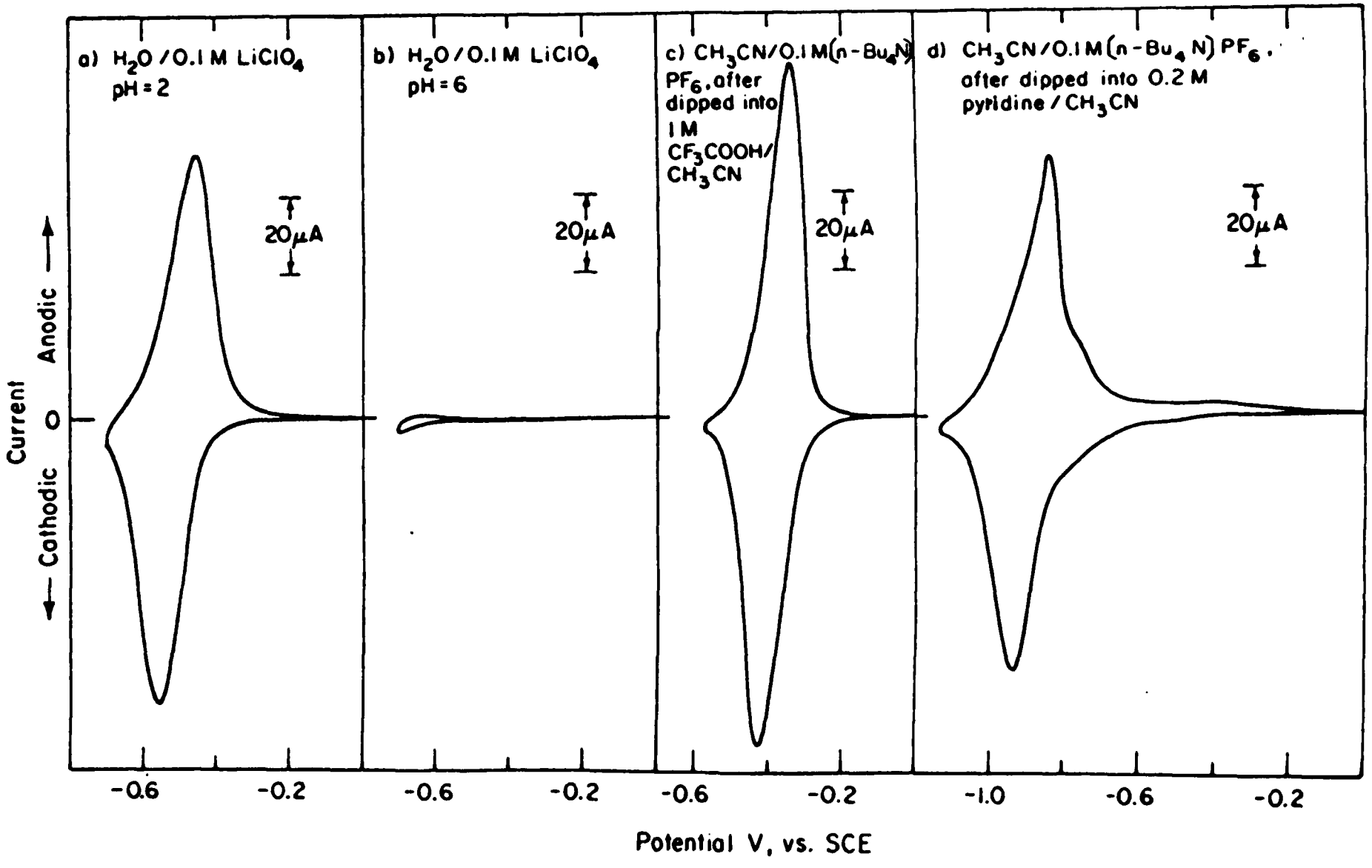
a) H_2O / 0.1 M $LiClO_4$
pH = 2
b) H_2O / 0.1 M $LiClO_4$
pH = 6
c) CH_3CN/0.1 M $(n\text{-}Bu_4N)PF_6$, after dipped into 1 M CF_3COOH/CH_3CN
d) CH_3CN/0.1 M $(n\text{-}Bu_4N)PF_6$, after dipped into 0.2 M pyridine / CH_3CN
20μA
Current
Anodic
Cathodic
0
-0.6
-0.2
-1.0
Potential V, vs. SCE

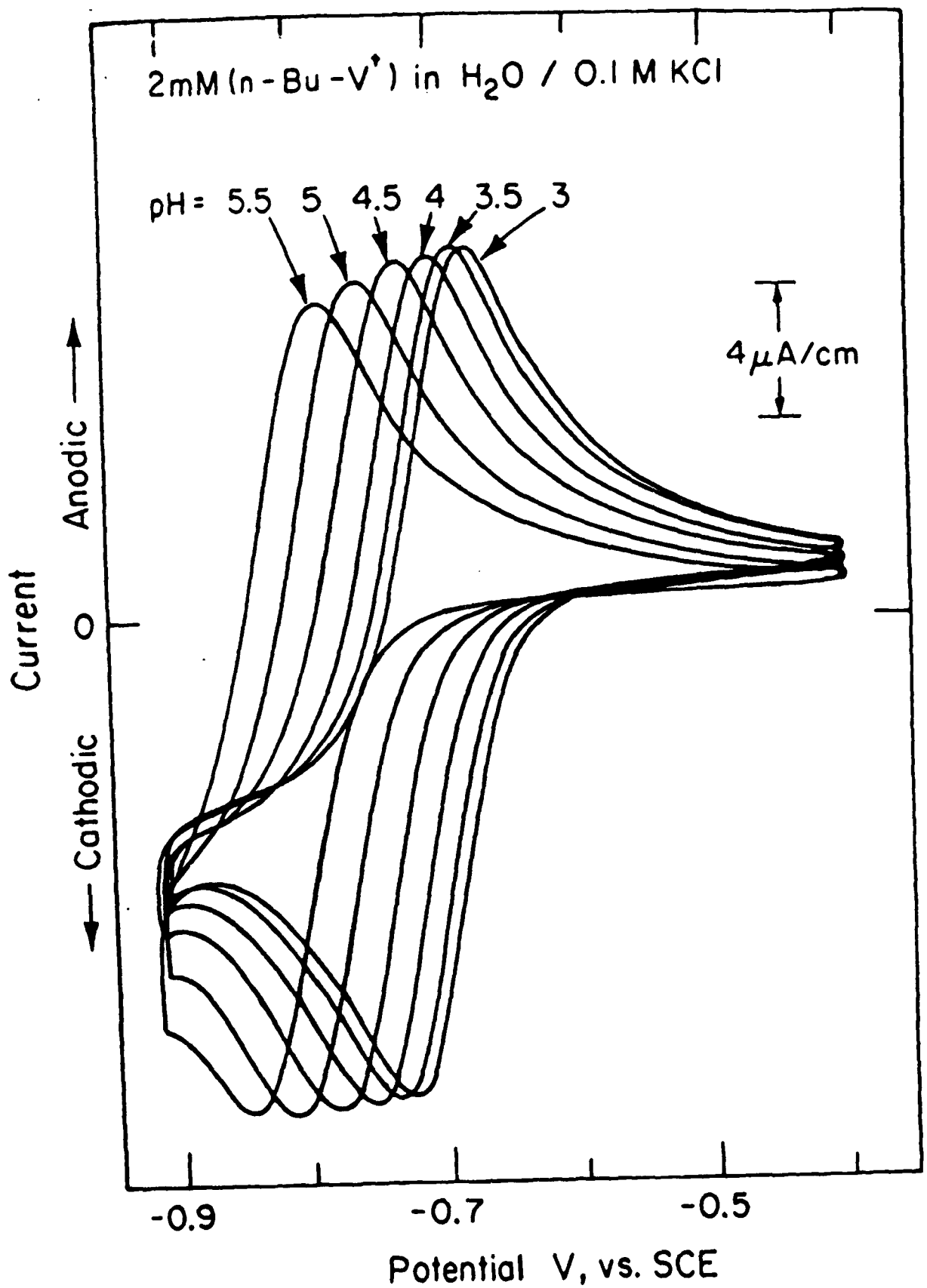
2mM (n-Bu-V^{+}) in H_2O / 0.1 M KCl
pH = 5.5 5 4.5 4 3.5 3
4 μA/cm
Current
Anodic
0
Cathodic
-0.9
-0.7
-0.5
Potential V, vs. SCE

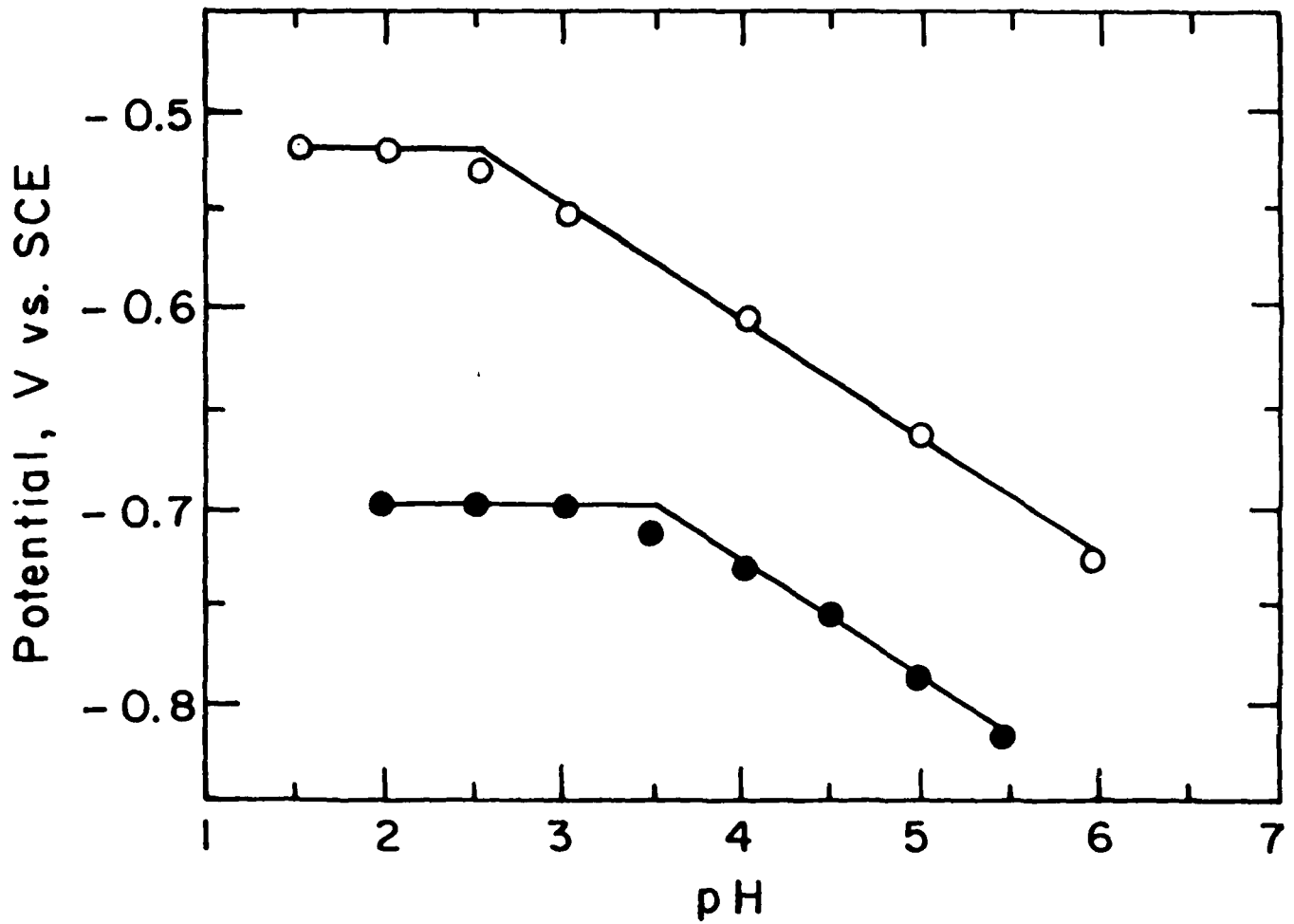
Potential, V vs. SCE
- 0.5
- 0.6
- 0.7
- 0.8
1
2
3
4
5
6
7
pH

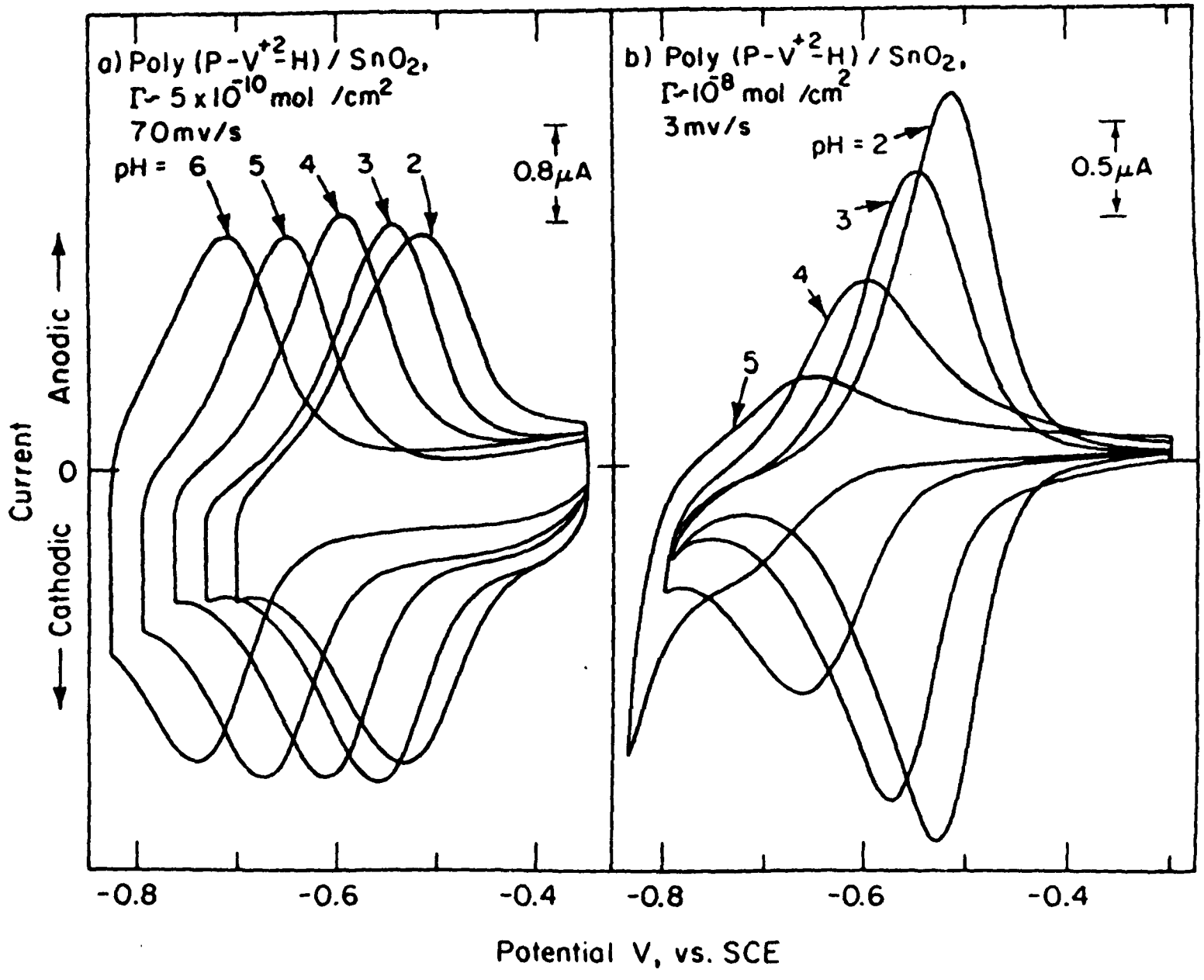
a) Poly (P-V+2-H) / SnO2,
Γ~ 5 x 10-10 mol /cm2
70mv/s
pH = 6 5 4 3 2
0.8μA
b) Poly (P-V+2-H) / SnO2,
Γ~10-8 mol /cm2
3mv/s
pH = 2
3
4
5
0.5μA
Current
Anodic
Cathodic
0
-0.8
-0.6
-0.4
-0.8
-0.6
-0.4
Potential V, vs. SCE

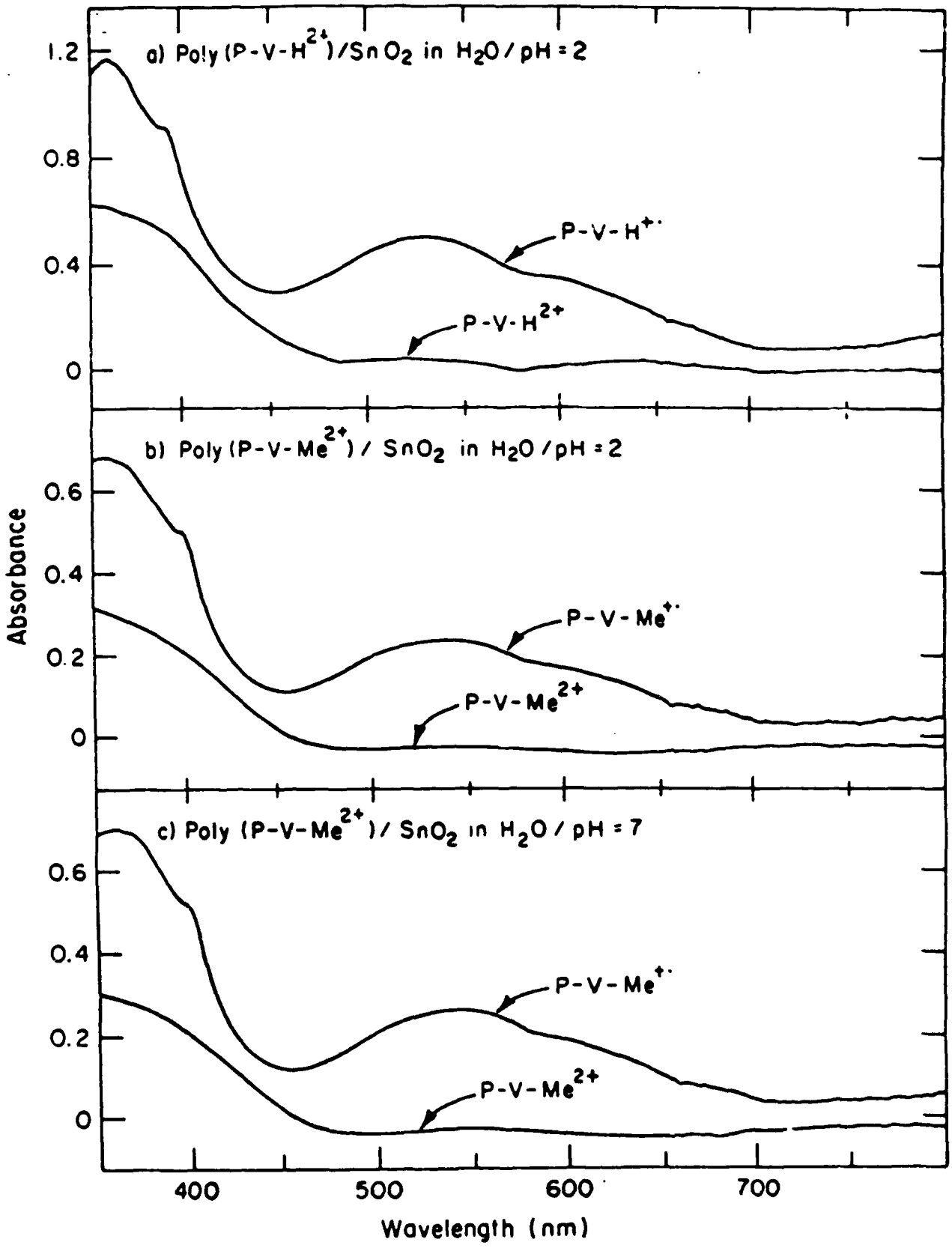
a) Poly (P-V-H^{2+}) / SnO_2 in H_2O / pH = 2
P-V-H$^{+\cdot}$
P-V-H^{2+}
b) Poly (P-V-Me^{2+}) / SnO_2 in H_2O / pH = 2
P-V-Me$^{+\cdot}$
P-V-Me^{2+}
c) Poly (P-V-Me^{2+}) / SnO_2 in H_2O / pH = 7
P-V-Me$^{+\cdot}$
P-V-Me^{2+}
Absorbance
1.2
0.8
0.4
0
0.6
0.4
0.2
0
0.6
0.4
0.2
0
400
500
600
700
Wavelength (nm)

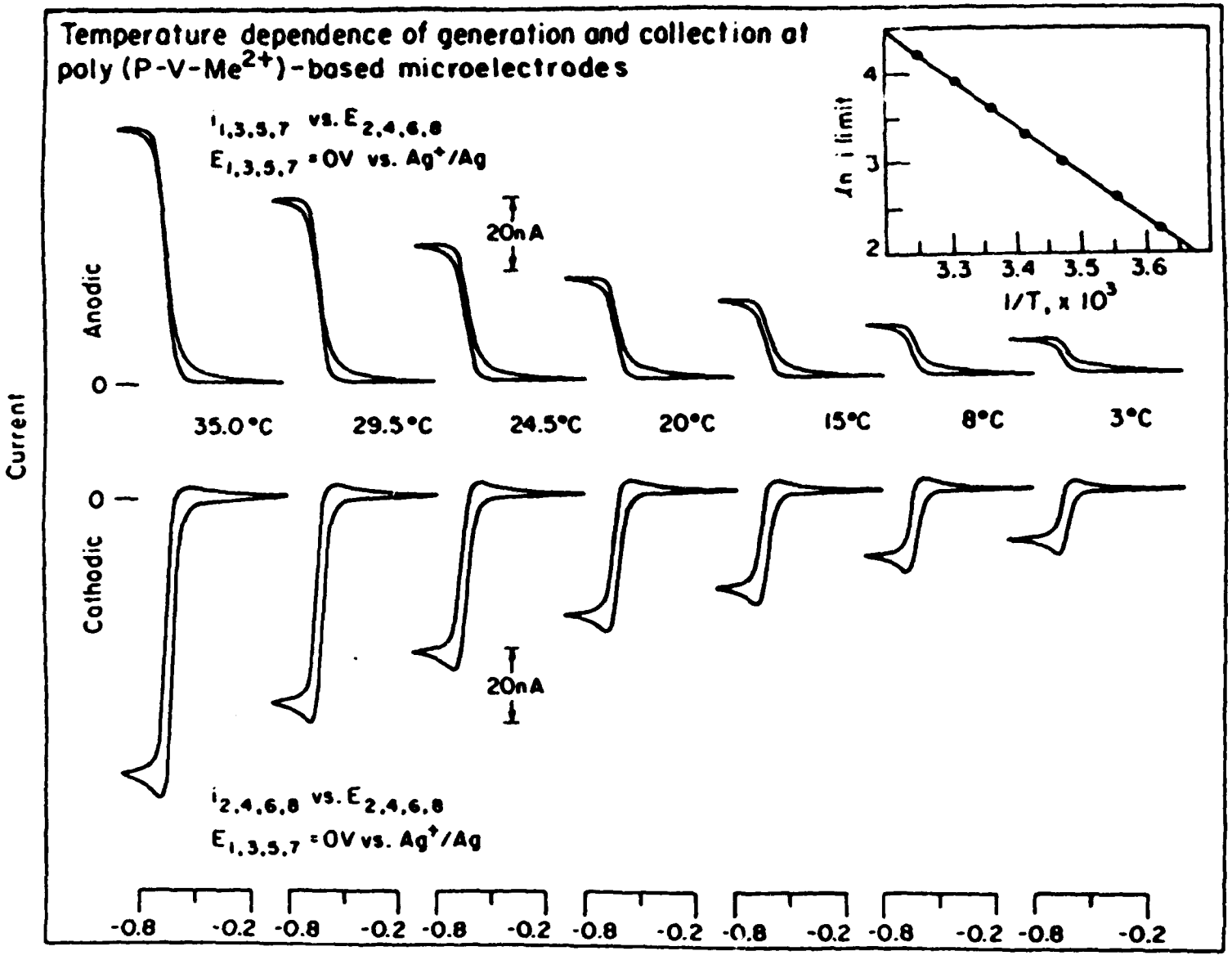
Temperature dependence of generation and collection at poly (P-V-Me2+)-based microelectrodes
i1,3,5,7 vs. E2,4,6,8
E1,3,5,7 = 0V vs. Ag+/Ag
20nA
Anodic
0
35.0°C
29.5°C
24.5°C
20°C
15°C
8°C
3°C
Current
0
Cathodic
20nA
i2,4,6,8 vs. E2,4,6,8
E1,3,5,7 = 0V vs. Ag+/Ag
-0.8 -0.2 -0.8 -0.2 -0.8 -0.2 -0.8 -0.2 -0.8 -0.2 -0.8 -0.2 -0.8 -0.2
Potential, V vs. Ag+/Ag
ln i limit
4
3
2
3.3 3.4 3.5 3.6
1/T, x 10³

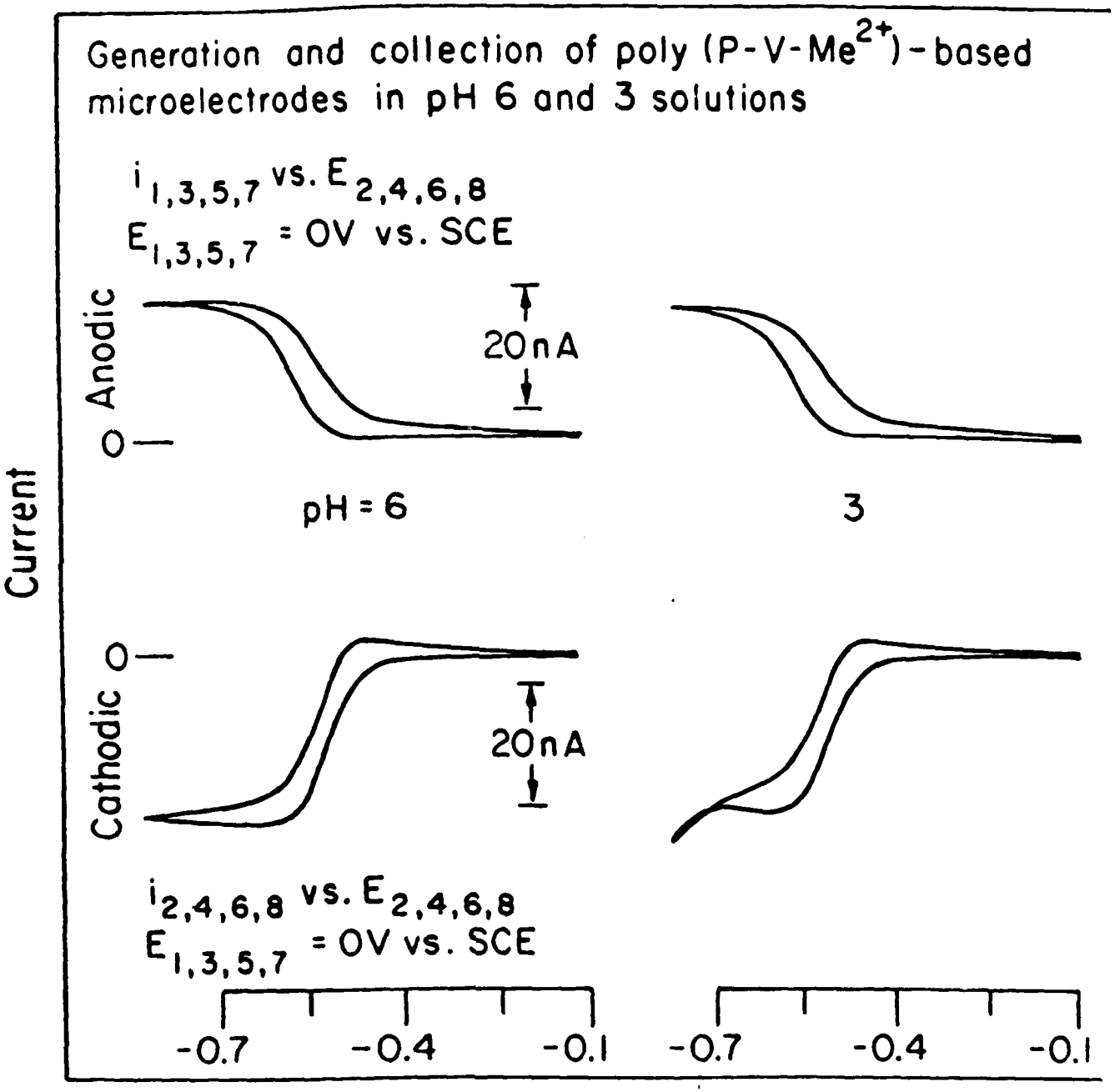
Generation and collection of poly (P-V-Me^{2+})-based microelectrodes in pH 6 and 3 solutions
$i_{1,3,5,7}$ vs. $E_{2,4,6,8}$
$E_{1,3,5,7}$ = OV vs. SCE
Anodic
0
20nA
pH = 6
3
Current
0
Cathodic
20nA
$i_{2,4,6,8}$ vs. $E_{2,4,6,8}$
$E_{1,3,5,7}$ = OV vs. SCE
-0.7
-0.4
-0.1
-0.7
-0.4
-0.1
Potential V, vs. SCE

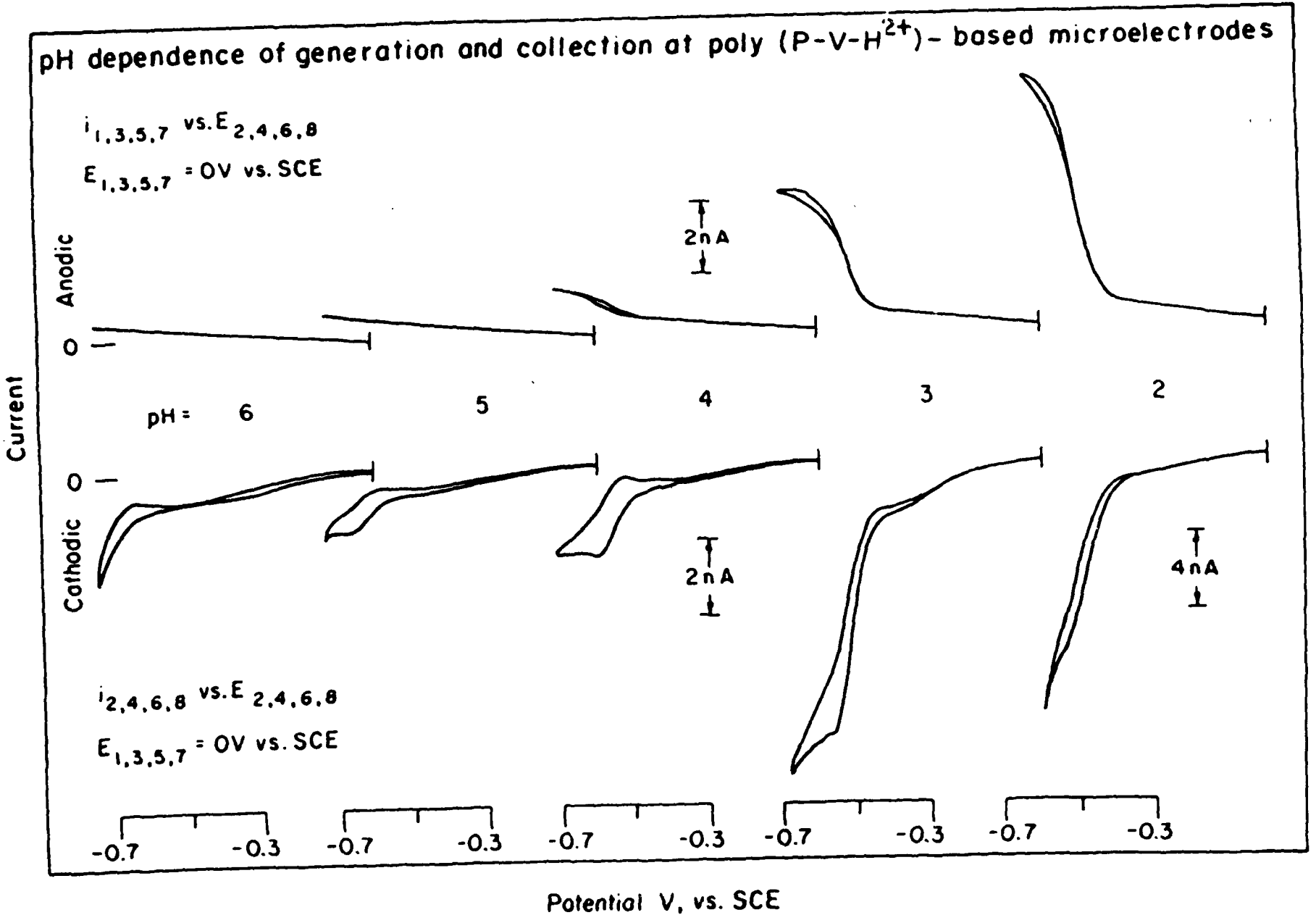
pH dependence of generation and collection at poly (P-V-H2+)- based microelectrodes
i1,3,5,7 vs. E2,4,6,8
E1,3,5,7 = OV vs. SCE
Anodic
0
2nA
pH = 6
5
4
3
2
Current
0
Cathodic
2nA
4nA
i2,4,6,8 vs. E2,4,6,8
E1,3,5,7 = OV vs. SCE
-0.7
-0.3
-0.7
-0.3
-0.7
-0.3
-0.7
-0.3
-0.7
-0.3
Potential V, vs. SCE

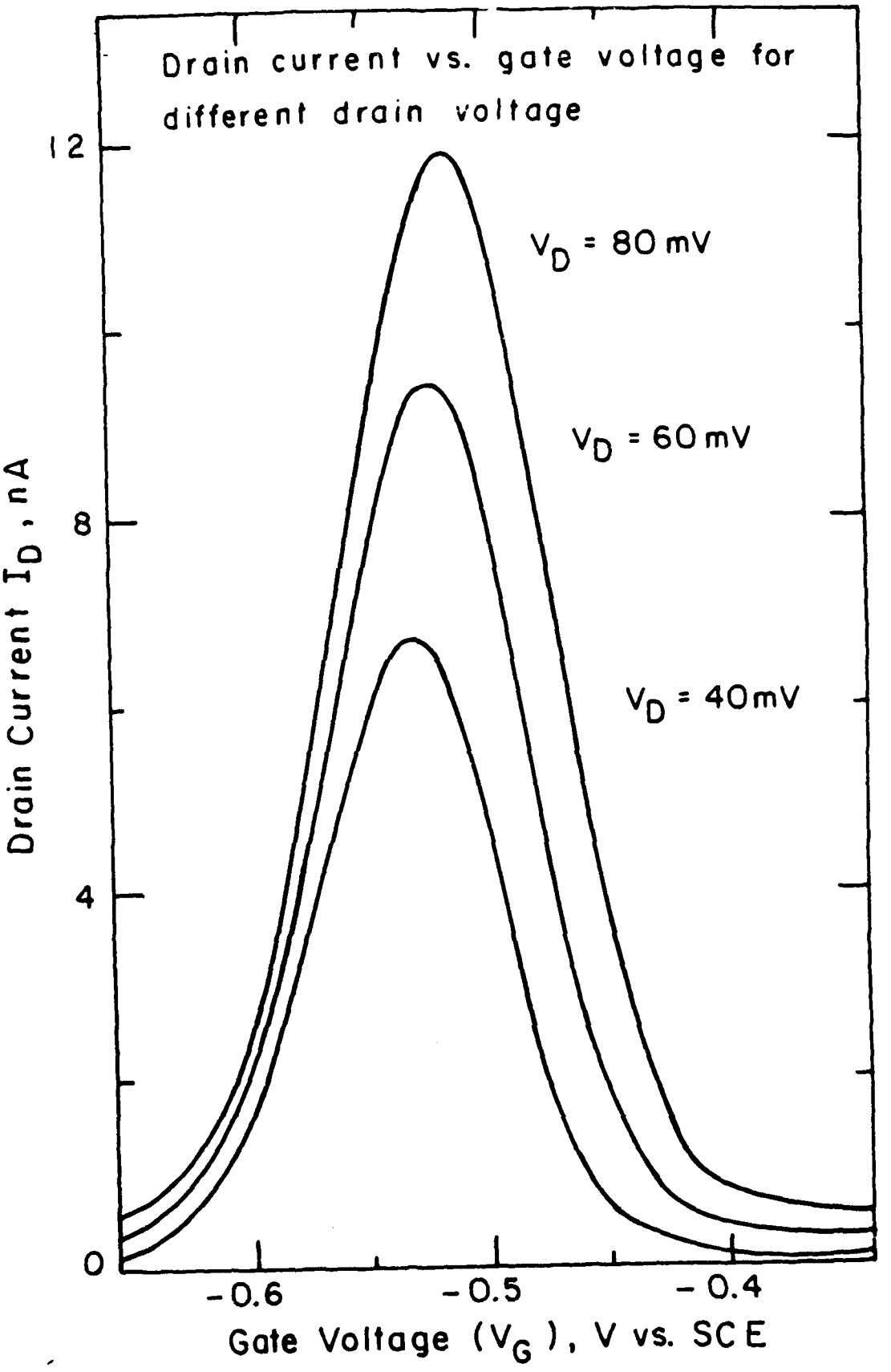
Drain current vs. gate voltage for different drain voltage
12
8
4
0
V_D = 80 mV
V_D = 60 mV
V_D = 40 mV
Drain Current I_D, nA
-0.6
-0.5
-0.4
Gate Voltage (V_G), V vs. SCE

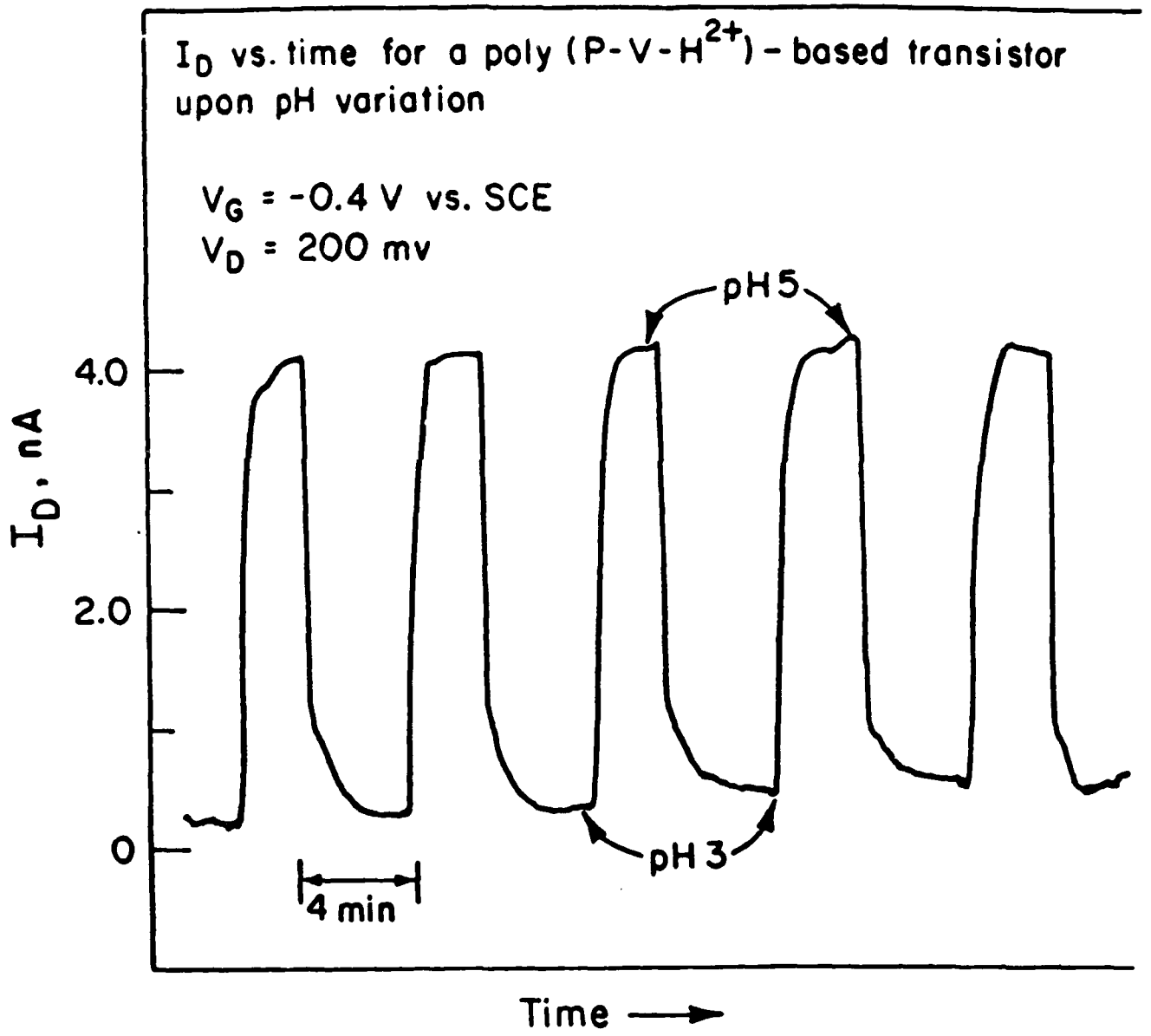
I_D vs. time for a poly (P-V-H^{2+}) - based transistor upon pH variation
V_G = -0.4 V vs. SCE
V_D = 200 mv
pH 5
pH 3
4.0
2.0
0
I_D, nA
4 min
Time

DL/1113/87/2

TECHNICAL REPORT DISTRIBUTION LIST, GEN

	No. Copies
Office of Naval Research Attn: Code 1113 800 N. Quincy Street Arlington, Virginia 22217-5000	2
Dr. Bernard Douda Naval Weapons Support Center Code 50C Crane, Indiana 47522-5050	1
Naval Civil Engineering Laboratory Attn: Dr. R. W. Drisko, Code L52 Port Hueneme, California 93401	1
Defense Technical Information Center Building 5, Cameron Station Alexandria, Virginia 22314	12 *high* quality
DTNSRDC Attn: Dr. H. Singerman Applied Chemistry Division Annapolis, Maryland 21401	1
Dr. William Tolles Superintendent Chemistry Division, Code 6100 Naval Research Laboratory Washington, D.C. 20375-5000	1
Dr. David Young Code 334 NORDA NSTL, Mississippi 39529	1
Naval Weapons Center Attn: Dr. Ron Atkins Chemistry Division China Lake, California 93555	1
Scientific Advisor Commandant of the Marine Corps Code RD-1 Washington, D.C. 20380	1
U.S. Army Research Office Attn: CRD-AA-IP P.O. Box 12211 Research Triangle Park, NC 27709	1
Mr. John Boyle Materials Branch Naval Ship Engineering Center Philadelphia, Pennsylvania 19112	1
Naval Ocean Systems Center Attn: Dr. S. Yamamoto Marine Sciences Division San Diego, California 91232	1